

---

---

## Gears — Calculation of load capacity of wormgears

*Engrenages — Calcul de la capacité de charge des engrenages à vis*

STANDARDSISO.COM : Click to view the full PDF of ISO/TR 14521:2010



**PDF disclaimer**

This PDF file may contain embedded typefaces. In accordance with Adobe's licensing policy, this file may be printed or viewed but shall not be edited unless the typefaces which are embedded are licensed to and installed on the computer performing the editing. In downloading this file, parties accept therein the responsibility of not infringing Adobe's licensing policy. The ISO Central Secretariat accepts no liability in this area.

Adobe is a trademark of Adobe Systems Incorporated.

Details of the software products used to create this PDF file can be found in the General Info relative to the file; the PDF-creation parameters were optimized for printing. Every care has been taken to ensure that the file is suitable for use by ISO member bodies. In the unlikely event that a problem relating to it is found, please inform the Central Secretariat at the address given below.

STANDARDSISO.COM : Click to view the full PDF of ISO/TR 14521:2010



**COPYRIGHT PROTECTED DOCUMENT**

© ISO 2010

All rights reserved. Unless otherwise specified, no part of this publication may be reproduced or utilized in any form or by any means, electronic or mechanical, including photocopying and microfilm, without permission in writing from either ISO at the address below or ISO's member body in the country of the requester.

ISO copyright office  
Case postale 56 • CH-1211 Geneva 20  
Tel. + 41 22 749 01 11  
Fax + 41 22 749 09 47  
E-mail [copyright@iso.org](mailto:copyright@iso.org)  
Web [www.iso.org](http://www.iso.org)

Published in Switzerland

# Contents

Page

Foreword .....	iv
Introduction.....	v
1 Scope .....	1
2 Normative references .....	1
3 Symbols and terminology.....	2
4 Formulae for calculation of dimensions .....	10
5 General .....	17
6 Geometrical data to be known for calculation .....	22
7 Forces, speeds and parameters for the calculation of stresses.....	24
8 Efficiency and power loss .....	32
9 Wear load capacity .....	38
10 Surface durability (pitting resistance).....	43
11 Deflection .....	45
12 Tooth root strength .....	47
13 Temperature safety factor .....	51
14 Determination of the wheel bulk temperature .....	54
Annex A (informative) Notes on physical parameters .....	57
Annex B (informative) Methods for the determination of the parameters .....	58
Annex C (informative) Lubricant film thickness according to EHL - theory .....	62
Annex D (informative) Wear path definitions .....	64
Annex E (informative) Notes on calculation wear .....	67
Annex F (informative) Notes on tooth root strength .....	68
Annex G (informative) The utilisation of existing tooling for machining of worm wheel teeth .....	69
Annex H (informative) Adaptation of equations for the reference gear to own results of measurements .....	72
Annex I (informative) Life time estimation for worm gears with a high risk of pitting damage.....	75
Annex J (informative) Examples.....	77
Bibliography.....	88

## Foreword

ISO (the International Organization for Standardization) is a worldwide federation of national standards bodies (ISO member bodies). The work of preparing International Standards is normally carried out through ISO technical committees. Each member body interested in a subject for which a technical committee has been established has the right to be represented on that committee. International organizations, governmental and non-governmental, in liaison with ISO, also take part in the work. ISO collaborates closely with the International Electrotechnical Commission (IEC) on all matters of electrotechnical standardization.

International Standards are drafted in accordance with the rules given in the ISO/IEC Directives, Part 2.

The main task of technical committees is to prepare International Standards. Draft International Standards adopted by the technical committees are circulated to the member bodies for voting. Publication as an International Standard requires approval by at least 75 % of the member bodies casting a vote.

In exceptional circumstances, when a technical committee has collected data of a different kind from that which is normally published as an International Standard ("state of the art", for example), it may decide by a simple majority vote of its participating members to publish a Technical Report. A Technical Report is entirely informative in nature and does not have to be reviewed until the data it provides are considered to be no longer valid or useful.

Attention is drawn to the possibility that some of the elements of this document may be the subject of patent rights. ISO shall not be held responsible for identifying any or all such patent rights.

ISO/TR 14521 was prepared by Technical Committee ISO/TC 60, *Gears*, Subcommittee SC 1, *Nomenclature and wormgearing*.

## Introduction

This Technical Report was developed for the rating and design of enclosed or open single enveloping worm gears with cylindrical worms, and worm-gearred motors having either solid or hollow output shafts.

This Technical Report is only applicable when the flanks of the worm wheel teeth are conjugate to those of the worm threads.

The particular shapes of the rack profiles from tip to root do not affect the conjugacy when the worm and worm wheel hobs have the same profiles; thus worm wheels have proper contact with worms and the motions of worm gear pairs are uniform.

This Technical Report can apply to worm gearing with cylindrical helicoidal worms having the following thread forms: A, C, I, N, K.

Other than the requirements of the three preceding paragraphs, no restrictions are placed on the manufacturing methods used.

In order to ensure proper mating and because of the many different thread profiles in use, it is generally desirable that worm and worm wheel be supplied by the same manufacturer.

In this Technical Report, the permissible torque for a worm gear is limited by considerations of surface stress (conveniently referred to as wear or pitting) or bending stress (referred to as strength) in both worm threads and worm wheel teeth, deflection of worm or thermal limitation.

Consequently, the load capacity of a pair of gears is determined using calculations concerned with all criteria described in the scope and 7.3. The permissible torque on the worm wheel is the least of the calculated values.

STANDARDSISO.COM : Click to view the full PDF of ISO/TR 14521:2010

# Gears — Calculation of load capacity of wormgears

**WARNING** — Special attention is required when establishing the tooth geometry especially for C type gear profile.

## 1 Scope

This Technical Report specifies equations for calculating the load capacity of cylindrical worm gears and covers load ratings associated with wear, pitting, worm deflection, tooth breakage and temperature. Scuffing and other failure modes are not covered by this Technical Report.

The load rating and design procedures are valid for sliding velocities over tooth surfaces of up to 25 m/s and contact ratios equal to or greater than 2,1. For wear, sliding velocities over tooth surfaces are not below 0,1 m/s.

The rules and recommendations for the dimensioning, lubricants or materials selected by this Technical Report only apply to centre distances of 50 mm and larger. For centre distances below 50 mm, method A applies.

The choice of appropriate methods of calculation requires knowledge and experience. This Technical Report is intended for use by experienced gear designers who are able to make informed judgements concerning factors. It is not intended for use by engineers who lack the necessary experience. See 5.4.

The geometry of worm gears is complex, therefore the user of this Technical Report is encouraged to make sure that a valid working geometry has been established.

## 2 Normative references

The following referenced documents are indispensable for the application of this document. For dated references, only the edition cited applies. For undated references, the latest edition of the referenced document (including any amendments) applies.

ISO 701:1998, *International gear notations — Symbols for geometrical data*

ISO 1122-2:1999, *Vocabulary of gear terms — Part 2: Definitions related to worm gears geometry*

ISO 6336-6, *Calculation of load capacity of spur and helical gear — Part 6: Calculation of service life under variable load*

ISO/TR 10828:1997, *Worm gears — Geometry of worm profiles*

DIN 3974-1:1995, *Accuracy of worms and wormgears — Part 1: General bases*

DIN 3974-2:1995, *Accuracy of worms and wormgears — Part 2: Tolerances for individual errors*

### 3 Symbols and terminology

#### 3.1 Symbols

NOTE Where applicable, the symbols are in accordance with ISO 701 and the definitions are in accordance ISO 1122-2.

**Table 1 — Symbols for worm gears**

Symbol	Description	Unit	Figure	Equation Number
$a$	centre distance	mm		38/39
$a_0, a_1, a_2$	oil sump temperature coefficients, calculated according to method C	-		160 to 166
$a_{\min}, a_{\max}$	minimum and maximum centre distance for tooling selection	mm		G.2/G.3
$a_T$	centre distance of standard reference gear	mm		
$b_1$	worm facewidth	mm		22
$b_2$	facewidth of the wheel as specified in DIN 3975	mm		36
$b_{2H}$	effective wheel facewidth	mm	Fig. 4	
$b_{2H, \text{std}}$	Standard worm wheel facewidth	mm		52
$b_{2R}$	wheel rim width	mm	Fig. 4	
$b_H$	half hertzian contact width	mm	Fig.19	
$c_1, c_2$	tip clearance	mm		
$c_1^*, c_2^*$	tip clearance coefficient in axial section	mm		
$c_{\text{oil}}$	specific heat capacity of the oil (for temperature calculation with spray lubrication)	Ws/(kg.K)		170
$c_\alpha$	proximity value for the viscosity pressure exponent $\alpha$	m <sup>2</sup> /N		64/66
$d_{a1}$	worm tip diameter	mm		13
$d_{a2}$	worm wheel tip diameter	mm		34
$d_{b1}$	base diameter of involute helicoid (for I profile)	mm		21
$d_{e2}$	worm wheel outside diameter	mm		35
$dF$	force transmitted by a segment of the contact line	N	Fig. B.2	B.3
$dl$	length of contact line segment	mm		B.1
$d_{f1}$	worm root diameter	mm		14
$d_{f2}$	worm wheel root diameter	mm		33
$d_{m1}$	worm reference diameter	mm	Fig. 2/5	9
$d_{m1T}$	reference diameter of the worm, from standard reference gear	mm		
$d_{m2}$	worm wheel reference diameter	mm	Fig 3/5	24
$d_{m2T}$	reference diameter of the wheel, from standard reference gear	mm		
$d_{w1}$	worm pitch diameter	mm		40
$d_{w2}$	worm wheel pitch diameter	mm		41
$e_{mx1}$	worm reference tooth space width in axial section	mm	Fig. 2	16
$e_{n1}$	worm normal tooth space width in normal section	mm		18



Table 1 (continued)

Symbol	Description	Unit	Figure	Equation Number
$e_{m2}$	worm wheel tooth space width in mid-plane section	mm		27
$f_h$	Worm wheel face width factor for the parameter for the minimum mean lubricant film thickness	-		58
$f_p$	Worm wheel face width factor for the parameter for the mean hertzian stress	-		59
$h_1$	worm tooth depth	mm		10
$h_2$	worm wheel tooth depth	mm		31
$h_{am1}$	worm tooth reference addendum in axial section	mm	Fig. 5	11
$h_{am2}$	worm wheel tooth reference addendum in mid-plane section	mm	Fig. 5	29
$h_{am1}^*$	worm tooth reference addendum coefficient in axial section	-		11
$h_{am2}^*$	worm wheel tooth reference addendum coefficient in mid-plane section	-		29
$h_{e2}$	worm wheel tooth external addendum	mm		32
$h_{fm1}$	worm tooth reference dedendum in axial section	mm		12
$h_{fm2}$	worm wheel tooth reference dedendum in mid-plane section	mm		30
$h_{fm1}^*$	worm tooth reference dedendum coefficient in axial section	-		
$h_{fm2}^*$	worm wheel tooth reference dedendum coefficient in mid-plane section	-		30
$h_{min}$	minimum lubricant film thickness	$\mu\text{m}$		C.1
$h_{min\ m}$	minimum mean lubricant film thickness	$\mu\text{m}$		63
$h^*$	parameter for minimum mean lubricant film thickness	-		56/57
$h_T^*$	parameter for minimum mean lubricant film thickness of the standard reference gear	-		
$j_x$	axial backlash	mm		
$k$	lubricant constant	1/K		69/71
$k^*$	mean heat transition coefficient	W/(m <sup>2</sup> ·K)		
$l_1$	spacing of the worm shaft bearings	mm		
$l_{11}, l_{12}$	bearing spacing of the worm shaft	mm	Fig. 11	
$m_{max}$	maximum axial module for tooling selection	mm	Fig. 11	G.4
$m_{min}$	minimum axial module for tooling selection	mm		G.5
$m_{xhob}$	axial module for tooling selection	mm		Annex G
$m_n$	normal module	mm		8
$m_{x\ 1}$	axial module	mm		2/G.1
$\Delta m$	material loss	mg		
$\Delta m_{lim}$	material loss limit	mg		
$n_1$	rotational speed of the worm shaft	min <sup>-1</sup>		
$n_2$	rotational speed of the wheel	min <sup>-1</sup>		
$N_S$	number of starts per hour			112

Table 1 (continued)

Symbol	Description	Unit	Figure	Equation Number
$p_0$	environmental pressure	N/mm <sup>2</sup>		
$p_{b1}$	base cylinder pitch for I profile	mm		22
$p_{Hm}$	hertzian stress; mean value for the total contact area	N/mm <sup>2</sup>		B.7
$p_m^*$	parameter for the mean hertzian stress	-		53/54
$p_{mT}^*$	parameter for the mean hertzian stress of the standard reference gear	-		
$p_{n1}$	normal pitch	mm		7
$p_{t2}$	transverse pitch	mm		25
$p_{x1}$	axial pitch	mm	Fig. 2	1
$p_{z1}$	lead of worm threads	mm		3
$q_1$	diameter factor	mm		4
$q_{hob}$	diameter factor for hob	mm		Annex G
$r_{g2}$	worm wheel throat radius	mm		37
$s_2$	reference tooth thickness of the wheel teeth in the spur section	mm		153
$s_{f2}$	mean tooth root thickness of the wheel teeth in the spur section	mm		153
$s_{ft2}$	mean tooth root thickness of the wheel teeth in the spur section	mm		153
$s_{gB}$	sliding path of the worm flanks within the hertzian contact of the wheel flank per number of cycles of the wheel, around the contact point (local value)	mm		D.3/D.5
$s_{gm}$	mean sliding path	mm		D.7
$s_{m2}$	tooth thickness at the reference diameter of the worm wheel	mm	Fig. 3	26
$s_K$	rim thickness	mm	Fig. 12	
$s_{Wm}$	wear path inside of the required life expectancy	mm		71/D.1
$s_{mx1}$	worm tooth thickness in axial section	mm	Fig. 2	15
$s_{mx1}^*$	worm tooth thickness in axial section coefficient	-		15
$s_{n1}$	normal worm tooth thickness in normal section	mm		17
$s^*$	parameter for the mean sliding path	-		59/60/D.8
$s_T^*$	parameter for the mean sliding path of the standard reference gear	-		
$\Delta s$	tooth thickness loss	mm		
$u$	gear ratio			42
$u_T$	gear ratio of the standard reference gear			
$v_1$	velocity of a flank point of the worm	m/s	Fig. B.1	62
$v_2$	velocity of a flank point of a worm wheel	m/s	Fig. B.1	62
$v_{1n}$	worm velocity component normal to the contact line	m/s	Fig. B.2	
$v_{2n}$	wheel velocity component normal to the contact line	m/s	Fig. B.2	
$\vec{V}_{gB}$	sliding velocity at the reference diameter in flank direction	m/s		91/92/93/E.6

Table 1 (continued)

Symbol	Description	Unit	Figure	Equation Number
$\bar{v}_g$	sliding velocity at mean reference diameter	m/s		51
$v_\Sigma$	sum velocity	m/s		53
$v_{\Sigma n}$	sum velocity in normal direction	m/s		53
$x_2$	worm wheel profile shift coefficient	-		28
$x_{2\max}$	maximum worm wheel profile shift coefficient for tooling selection	-		H.3
$x_{2\min}$	minimum worm wheel profile shift coefficient for tooling selection	-		H.3
$z_1$	number of threads in worm	-		
$z_2$	number of teeth in worm wheel	-		
$A$	coefficient for kinematic viscosity			76
$A_{\text{ges}}$	free surface of the gear housing	m <sup>2</sup>		
$A_{\text{fl}}$	total flank surface of the worm wheel	mm <sup>2</sup>		131
$A_R$	dominant cooled surface of the gear set	m <sup>2</sup>		174
$B$	coefficient for kinematic viscosity	-		76
$c$	immersion factor	-		
$E_1$	modulus of elasticity of the worm	N/mm <sup>2</sup>		
$E_2$	modulus of elasticity of the worm wheel	N/mm <sup>2</sup>		
$E_{\text{red}}$	equivalent modulus of elasticity	N/mm <sup>2</sup>		62
$E_{\text{steel}}$	modulus of elasticity for steel	N/mm <sup>2</sup>		62
$F_{\text{xm1}}$	axial force to the worm shaft	N		46/49
$F_{\text{xm2}}$	axial force to the worm wheel	N		45/48
$F_{\text{rm1}}$	radial force to the worm shaft	N		47
$F_{\text{rm2}}$	radial force to the worm wheel	N		53
$F_{\text{tm1}}$	circumferential or tangential force to the worm shaft	N		45/48
$F_{\text{tm2}}$	circumferential or tangential force to the worm wheel	N		46/49
$dF/db$	specific loading	N/mm		
$J_{\text{OT}}$	reference wear intensity	-	Fig. 10	111 to 121
$J_W$	wear intensity	-		110
$K_n$	rotational speed factor / wheel bulk temperature	-		177
$K_{H\alpha}$	transverse load distribution factor	-		
$K_{H\beta}$	longitudinal load distribution factor	-		
$K_S$	size factor / wheel bulk temperature	-		179
$K_A$	application factor	-		
$K_V$	dynamic factor	-		
$K_W$	lubricant film thickness parameter	-		122
$K_v$	viscosity factor / wheel bulk temperature	-		178
$L_h$	life time	h		
$N_L$	number of stress cycles of the worm wheel	-		73
$P_1$	input power to the worm shaft	W		

Table 1 (continued)

Symbol	Description	Unit	Figure	Equation Number
$P_2$	output power from the worm wheel shaft	W		
$P_K$	cooling capacity of the oil with spray lubrication	W		169
$P_V$	total power loss of the worm gear unit	W		80
$P_{VO}$	idle running power loss	W		80/81/H.1
$P_{VZ1-2}$	meshing power loss in reducer	W		104
$P_{VZ2-1}$	meshing power loss in increaser	W		106
$P_{VD}$	sealing power loss	W		86/87
$P_{VLP}$	bearing power loss through loading	W		82 to 85
$Q_{oil}$	spray quantity	m <sup>3</sup> /s		
$Ra_1$	arithmetic mean roughness	µm		
$Ra_T$	arithmetic mean roughness for reference gear	µm		80
$Rz_1$	mean roughness depth	µm		
$S_F$	tooth breakage safety factor	-		148
$S_{F \min}$	minimum tooth breakage safety factor	-		149
$S_H$	pitting safety factor	-		133
$S_T$	temperature safety factor	-		157/167
$S_{T \min}$	minimum temperature safety factor	-		158/168
$S_W$	wear safety factor	-		107
$S_{W \min}$	minimum wear safety factor	-		108
$S_\delta$	deflection safety factor	-		143
$S_{\delta \lim}$	limit of deflection safety factor	-		144
$T_1$	input torque to the worm shaft	Nm		43
$T_{1N}$	nominal input torque to the worm shaft	Nm		43
$T_2$	output torque from the worm wheel	Nm		44/B.4/ B.5
$T_{2N}$	nominal output torque from the worm wheel	Nm		44
$W_H$	pressure factor	-		126/127
$W_{ML}$	material – lubricant factor	-		
$W_{NS}$	start factor	-		125
$W_S$	lubricant structure factor	-		123/124
$Y_F$	form factor / tooth breakage	-		151/152
$Y_G$	geometry factor / coefficient of friction	-		101/102
$Y_K$	rim thickness factor / tooth breakage	-		155
$Y_{NL}$	life factor / tooth breakage	-	Fig 13a/b	Table 11
$Y_R$	roughness factor / coefficient of friction	-		103/104
$Y_S$	size factor / coefficient of friction	-		99/100
$Y_W$	material factor / coefficient of friction	-		
$Y_\varepsilon$	contact factor / tooth breakage	-		151
$Y_\gamma$	lead factor / tooth breakage	-		154
$Z_h$	life factor / pitting	-		136

Table 1 (continued)

Symbol	Description	Unit	Figure	Equation Number
$Z_{oil}$	lubricant factor / pitting	-		142
$Z_S$	size factor / pitting	-		138/139
$Z_u$	gear ratio factor	-		141/142
$Z_v$	velocity factor / pitting	-		137
$\alpha$	pressure viscosity factor	m <sup>2</sup> /N		
$\alpha_{ot}$	axial pressure angle for A profile	°		
$\alpha_L$	heat transition coefficient for immersed wheel teeth	W/(m <sup>2</sup> K)		175
$\alpha_n$	normal pressure angle	°		19
$\beta_{m1}$	reference helix angle of worm	°		6
$\gamma_{m1}$	reference lead angle of worm	°		5
$\gamma_{b1}$	base lead angle of worm thread (for I profile)	°		19
$\delta_{lim}$	limiting value of deflection	mm		147
$\delta_m$	incurred deflection	mm		145/146
$\delta_{Wn}$	flank loss from wheel through abrasive wear in the normal section	mm		109
$\delta_{W lim}$	limiting value of flank loss	mm		132
$\delta_{W lim n}$	limiting value of flank loss in normal section	mm		128 to 130
$\eta_{ges}$	total efficiency in reducer	-		77
$\eta'_{ges}$	total efficiency in increaser	-		78
$\eta_{z1-2}$	gear efficiency in reducer	-		88
$\eta_{z2-1}$	gear efficiency in increaser	-		89
$\eta_{0M}$	dynamic viscosity of lubricant at ambient pressure and wheel bulk temperature	Ns/m <sup>2</sup>		67
$\theta$	temperature	°C		
$\Delta\theta$	temperature difference between oil sump and worm wheel bulk temperature	°C		173
$\theta_{in}$	oil entrance temperature	°C		
$\theta_{out}$	oil exit temperature	°C		
$\theta_0$	ambient temperature	°C		
$\theta_{oil}$	spray temperature	°C		
$\Delta\theta_{oil}$	oil temperature difference between input and output cooling system	°C		171
$\theta_M$	wheel bulk temperature	°C		172/176
$\theta_S$	oil sump temperature	°C		159/161
$\theta_{S lim}$	limiting value of oil sump temperature	°C		
$\mu_{0T}$	base coefficient of friction	-		91 to 93
$\mu_{zm}$	mean tooth coefficient of friction	-		90
$\nu_1$	POISSON ratio of the worm	-		
$\nu_2$	POISSON ratio for the worm wheel	-		
$\nu_\theta$	kinematic viscosity at oil temperature $\theta$	mm <sup>2</sup> /s		74
$\nu_{40}$	kinematic viscosity at 40 °C	mm <sup>2</sup> /s		74

Table 1 (continued)

Symbol	Description	Unit	Figure	Equation Number
$\nu_{100}$	kinematic viscosity at 100 °C	mm <sup>2</sup> /s		
$\nu_M$	kinematic viscosity at wheel bulk temperature	mm <sup>2</sup> /s		67
$\rho$	profile radius of the grinding disk for C type	mm		
$\rho_{oil}$	lubricant density	kg/dm <sup>3</sup>		
$\rho_{oil15}$	lubricant density at 15 °C	kg/dm <sup>3</sup>		68
$\rho_{oilM}$	lubricant density at wheel bulk temperature	kg/dm <sup>3</sup>		67
$\rho_{red}$	equivalent radius of curvature	mm		B.2
$\rho_z$	friction angle for the tooth coefficient of friction	°		
$\rho_{Rad}$	material density of the wheel	mg/mm <sup>3</sup>		
$\Delta_s \lim$	allowable tooth thickness loss	mm		129
$\sigma_{H \lim T}$	pitting strength	N/mm <sup>2</sup>		
$\sigma_H$	contact stress	N/mm <sup>2</sup>		135
$\sigma_{Hm}$	mean contact stress	N/mm <sup>2</sup>		61
$\sigma_{HG}$	limiting value for the mean contact stress	N/mm <sup>2</sup>		135
$\tau_F$	shear stress at tooth root	N/mm <sup>2</sup>		150
$\tau_{F \lim T}$	shear endurance strength	N/mm <sup>2</sup>		
$\tau_{FG}$	limiting value for shear stress at tooth root	N/mm <sup>2</sup>		156
$\omega_2$	angular velocity	s <sup>-1</sup>		

### 3.2 Worm gear load capacity rating criteria

The load capacity of a worm gear corresponds to the torque (or the power) which can be transmitted without the occurrence of tooth breakage or the appearance of excessive damage on the active flanks of the teeth during the design life of the gearing.

The following conditions can limit the rated load capacity:

- **wear:** damage usually appears on the tooth flanks of bronze worm wheels and is also influenced by the number of starts per hour,
- **pitting:** this form of damage may appear on the flanks of worm wheel teeth. Its development is strongly influenced by the load transmitted and the load-sharing conditions,
- **tooth breakage:** shear failure of worm wheel teeth or worm threads can occur when teeth become thin due to wear or overload,
- **worm thread and worm shaft breakage:** shaft breakage can occur as a result of bending fatigue or overload,
- **worm shaft deflection:** excessive deformation under load modifying contact pattern between worm and worm wheel,
- **scuffing:** this form of damage often appears suddenly. It is strongly influenced by transmitted load, sliding velocities and the conditions of lubrication,
- **working temperature:** when excessively high working temperature leads to accelerated degradation of the worm gear lubricant,
- **type of limitations in worm gear rating:** Table 2 indicates the relationship between different forms of capacity limits in combination with speed and torque.

When the many influence factors such as material properties, meshing conditions, (e.g. contact pattern under load), lubrication and etc. are considered, it is apparent that values of Hertzian pressure along the lines of contact are extremely significant.

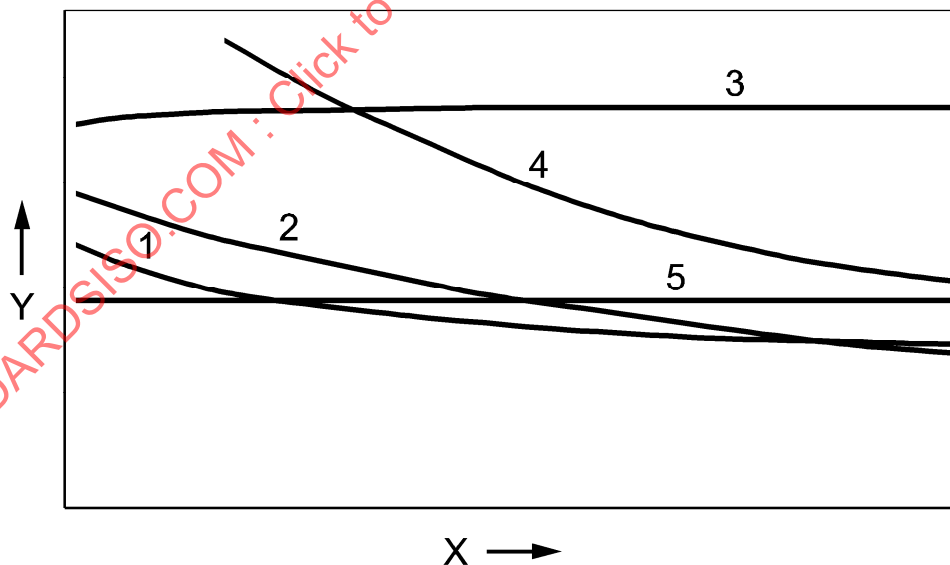
The different rating criteria are calculated independently and not in combination (see Figure 1). For a given worm gear pair, the zone of contact could change with loading. At a steady load, fatigue pits can develop which may subsequently be reduced by wear. This can be followed by further pitting, additional wear or a stable condition.

The most significant factors of gear tooth damage are shown in the first column of Table 2.

The load capacity of worm gearing is determined by calculations dealing with permissible stresses for pitting and wear, the deflection in worm, shafts, and the temperature. The permissible torque shall be determined from the least of the calculated values.

**Table 2 — Most significant factors: failure mode according to influence factors**

Influence factors	Failure modes					
	Wear	Pitting	Tooth-Breakage	Worm shaft Deflection	Scuffing	Low efficiency
Hertzian pressure	x	x	x	x	x	x
Worm speed	x	x			x	x
Oil film thickness	x	x			x	x
Oil	x	x			x	x
Contact Pattern	x	x	x		x	x
Worm surface roughness	x	x			x	x
Shearing value			x			

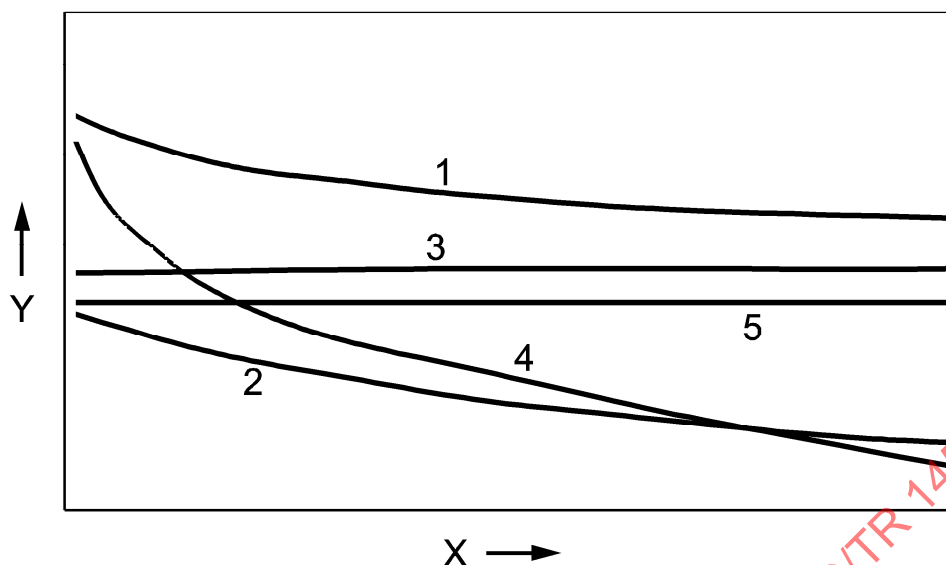


**Key**

- 1 wear
- 2 pitting
- 3 worm shaft deflection
- 4 temperature
- 5 tooth breakage

- X worm speed  $n_1$
- Y output torque  $T_2$

**Figure 1a — Example for small center distance**

**Key**

- 1 wear
- 2 pitting
- 3 worm shaft deflection
- 4 temperature
- 5 tooth breakage

- X worm speed  $n_1$
- Y output torque  $T_2$

Figure 1b — Example for large centre distance

Figure 1 — Limitations of worm gear torque

**3.3 Basis of the method**

The calculation methods are partly based on investigations of test gears (see, standard reference gear, 5.2), and partly on application experience. Investigations on test gears are mainly ascertained through varied test conditions and verified through practical experience. They are not however physically justified.

**4 Formulae for calculation of dimensions****4.1 Parameters for a cylindrical worm****4.1.1 Axial pitch**

$$p_{x1} = \pi \cdot m_{x1} \quad (1)$$

**4.1.2 Axial module**

$$m_{x1} = \frac{p_{x1}}{\pi} \quad (2)$$

**4.1.3 Lead**

$$p_{z1} = z_1 \cdot p_{x1} \quad (3)$$



#### 4.1.4 Diametral factor

$$q_1 = \frac{d_{m1}}{m_{x1}} \quad (4)$$

#### 4.1.5 Reference lead angle

$$\tan \gamma_{m1} = \frac{m_{x1} \cdot z_1}{d_{m1}} = \frac{z_1}{q_1} \quad (5)$$

#### 4.1.6 Reference helix angle

$$\beta_{m1} = 90^\circ - \gamma_{m1} \quad (6)$$

#### 4.1.7 Normal pitch on reference cylinder

$$p_{n1} = p_{x1} \cdot \cos \gamma_{m1} \quad (7)$$

#### 4.1.8 Normal module

$$m_n = m_{x1} \cdot \cos \gamma_{m1} \quad (8)$$

#### 4.1.9 Reference diameter

$$d_{m1} = q_1 \cdot m_{x1} \quad (9)$$

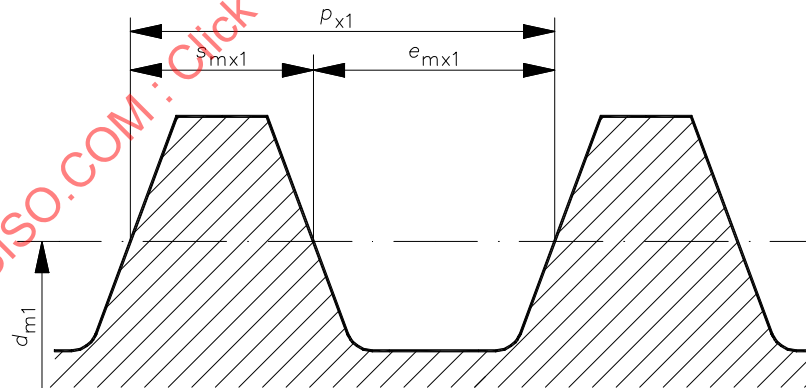


Figure 2 — Axial pitch, reference tooth thickness and reference tooth space for worm

#### 4.1.10 Reference tooth depth

$$h_1 = h_{am1} + h_{fm1} = \frac{1}{2} \cdot (d_{a1} - d_{f1}) \quad (10)$$

#### 4.1.11 Reference addendum

$$h_{a1} = h_{a1}^* \cdot m_{x1} = \frac{1}{2} \cdot (d_{a1} - d_{m1}) \quad (11)$$

where  $h_{a1}^*$  is the addendum coefficient = 1 (normally)

#### 4.1.12 Reference dedendum

$$h_{f1} = h_{f1}^* \cdot m_{x1} = \frac{1}{2} \cdot (d_{m1} - d_{f1}) \quad (12)$$

where  $h_{f1}^*$  = dedendum coefficient; generally  $1,1 < h_{f1}^* < 1,3$ , the recommended value is 1,2

#### 4.1.13 Tip diameter

$$d_{a1} = d_{m1} + 2 \cdot h_{a1} \quad (13)$$

#### 4.1.14 Root diameter

$$d_{f1} = d_{m1} - 2 \cdot h_{f1} \quad (14)$$

#### 4.1.15 Tooth thickness coefficient $s_{mx1}^*$

A recommended value is  $s_{mx1}^* = 0,5$

In general practice, this coefficient is very often less than 0,5 when there is a wish to increase the worm wheel tooth thickness to prevent wear of bronze and to increase strength of worm wheel.

See Figure 2

#### 4.1.16 Reference tooth thickness in the axial section

$$s_{mx1} = s_{mx1}^* \cdot p_{x1} \quad (15)$$

#### 4.1.17 Reference space width in the axial section

$$e_{mx1} = p_{x1} - s_{mx1} \quad (16)$$

#### 4.1.18 Normal tooth thickness

$$s_{n1} = s_{mx1} \cdot \cos \gamma_{m1} \quad (17)$$

#### 4.1.19 Normal space width

$$e_{n1} = e_{mx1} \cdot \cos \gamma_{m1} \quad (18)$$

**4.1.20 Profile flank form**

It is specified by a letter:

A is the straight sided axial thickness section

N is the straight sided normal space width section

I is the involute helicoid

K is the milled helicoid by double cone form

C is the milled helicoid by circular convex form

**4.1.21 Normal pressure angle**

$$\tan \alpha_n = \tan \alpha_{ot} \cdot \cos \gamma_{m1} \quad (19)$$

NOTE 1 For I, N, K, C profiles  $\alpha_n = \alpha_{on}$  defined in ISO 10828

NOTE 2 For A profile  $\alpha_n$  is defined by Equation (19)

**4.1.22 Base lead angle for I profile**

$$\cos \gamma_{b1} = \cos \gamma_{m1} \cdot \cos \alpha_n \quad (20)$$

**4.1.23 Base diameter for I profile**

$$d_{b1} = d_{m1} \cdot \frac{\tan \gamma_{m1}}{\tan \gamma_{b1}} = \frac{m_{x1} \cdot z_1}{\tan \gamma_{b1}} \quad (21)$$

**4.1.24 Base cylinder pitch for I profile**

$$p_{b1} = p_{x1} \cdot \cos \gamma_{b1} \quad (22)$$

**4.1.25 Worm face width**

$$b_1 \geq \sqrt{(d_{e2})^2 - (2 \cdot a - d_{a1})^2} \quad (23)$$

**4.2 Parameters for a worm wheel****4.2.1 Reference diameter**

$$d_{m2} = d_{w2} + 2 \cdot x_2 \cdot m_{x1} \text{ or } d_{m2} = 2 \cdot a - d_{m1} \quad (24)$$

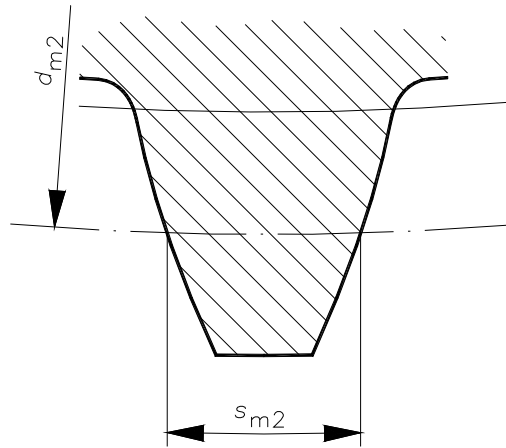


Figure 3 — Tooth thickness for worm wheel

#### 4.2.2 Transverse pitch

$$p_{t2} = p_{x1} \quad (25)$$

#### 4.2.3 Transverse tooth thickness at reference diameter

This value can be calculated only for a worm wheel without addendum modification as follows:

$$s_{m2} = e_{mx1} - j_x \quad (26)$$

where  $j_x$  = axial backlash

See Figure 3.

#### 4.2.4 Space width at reference diameter

$$e_{m2} = p_{x1} - s_{m2} \quad (27)$$

#### 4.2.5 Profile shift coefficient

$$x_2 = \frac{2 \cdot a - d_{m1} - m_{x1} \cdot z_2}{2 \cdot m_{x1}} \quad (28)$$

#### 4.2.6 Addendum

$$h_{am2} = m_{x1} \cdot h_{am2}^* = \frac{1}{2} \cdot (d_{a2} - d_{m2}) \quad (29)$$

where  $h_{am2}^*$  is the addendum coefficient;  $h_{am2}^* = 1$  (normally).

#### 4.2.7 Dedendum

$$h_{fm2} = m_{x1} \cdot h_{fm2}^* = \frac{1}{2} \cdot (d_{m2} - d_{f2}) \quad (30)$$

where  $h_{fm2}^*$  is the dedendum coefficient; generally  $1,1 < h_{fm2}^* < 1,3$ , the recommended value is 1,2.

**4.2.8 Tooth depth**

$$h_2 = h_{am2} + h_{fm2} \quad (31)$$

**4.2.9 Outside addendum**

$$h_{e2} = \frac{1}{2} \cdot (d_{e2} - d_{a2}) \quad (32)$$

Generally:  $0,4 \leq \frac{h_{e2}}{m_{x1}} \leq 1,5$

Normally:  $h_{e2}/m_{x1} = 0,5$

**4.2.10 Root diameter**

$$d_{f2} = d_{m2} - 2h_{fm2} \quad (33)$$

**4.2.11 Tip diameter**

$$d_{a2} = d_{m2} + 2h_{am2} \quad (34)$$

**4.2.12 Outside diameter**

$$d_{e2} = d_{a2} + 2 \cdot h_{e2} \quad (35)$$

**4.2.13 Worm wheel face width**

$$b_{2H \max} = \sqrt{(2 \cdot a - d_{f2})^2 - (2 \cdot a - d_{e2})^2} \quad (36)$$

See Figure 4.

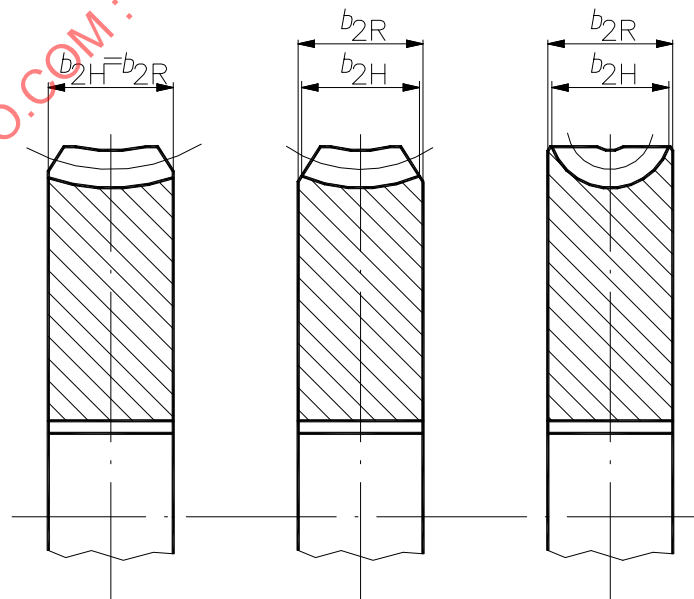


Figure 4 — Worm wheel face width

#### 4.2.14 Throat radius

$$r_{g2} \geq a - \frac{d_{a2}}{2} \quad (37)$$

### 4.3 Meshing parameters

#### 4.3.1 Centre distance

$$a = 0,5 \cdot (d_{m1} + d_{m2}) = 0,5 \cdot (d_{w1} + d_{w2}) \quad (38)$$

or

$$a = m_{x1} \cdot [0,5 \cdot (q_1 + z_2) + x_2] \quad (39)$$

See Figure 5.

#### 4.3.2 Pitch diameter for worm wheel

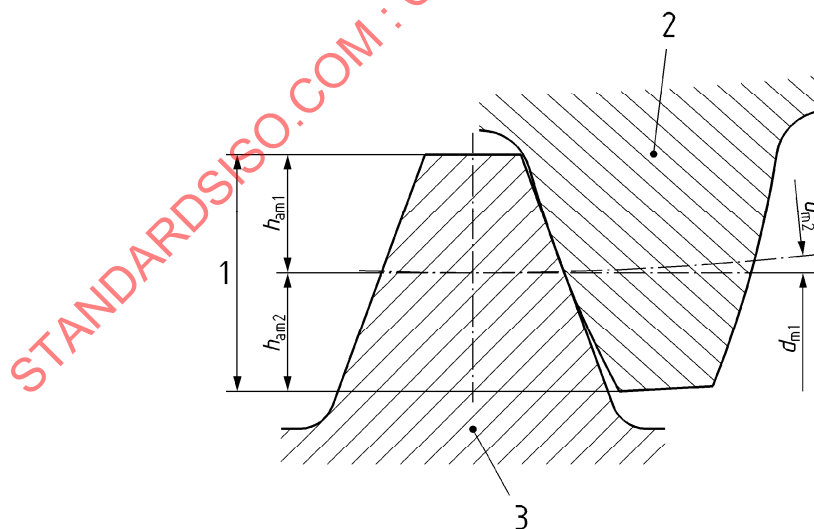
$$d_{w2} = z_2 \cdot m_{x1} \quad (40)$$

#### 4.3.3 Pitch diameter for worm

$$d_{w1} = 2 \cdot a - d_{w2} \quad (41)$$

#### 4.3.4 Worm gear ratio

$$u = \frac{z_2}{z_1} \quad (42)$$



#### Key

- 1 working depth
- 2 wheel
- 3 worm

Figure 5 — Reference diameters for worm gears ( $h_{am1} = h_{am2}$ )

#### 4.3.5 Contact ratio

The calculation of the contact ratio is out of the scope of this standard. The definition of contact ratio is according to ISO 1122-2.

#### 4.3.6 Relation to cutting tool parameters

See Annex G

### 5 General

The equations used for the calculation procedure in this Technical Report lead to either an absolute form (calculation with absolute parameters) or to a relative form (calculation with relative parameters).

**Absolute parameters:** The calculation is used when no specific tests are available. The precision of the gear calculations is improved as the differences concerning geometric dimensions, the operating conditions, material and lubricant, to those taken from the standard reference gears are decreased.

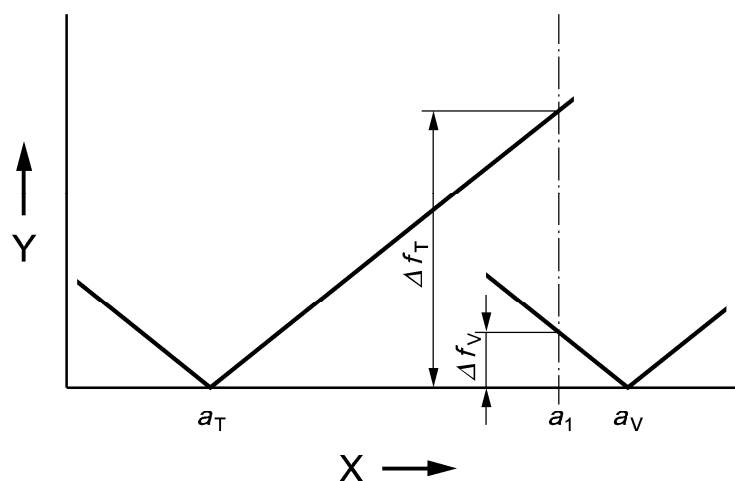
**Relative parameters:** The calculation offers the possibility to use investigation results in the corresponding calculation process directly. This enables the calculation procedure of the specific results to be adapted.

As the gear to be calculated concerning dimensions, materials, lubricants and operating conditions approach those for the standard reference gear or, if the corresponding test gear data is available, the deviation is decreased. Figure 6 shows an example of influence of centre distance.

The gear concerned has a centre distance of  $a_1$ , which is clearly a deviation from that of the standard reference gear  $a_T$ . Thus a relative deviation  $\Delta f_T$  is given. Furthermore test results are available for a gear with centre distance of  $a_V$ . In calibrating the calculation procedure to this centre distance a deviation of  $\Delta f_V$  is yielded (by linear regression). This deviation is significantly smaller than the deviation  $\Delta f_T$ , since the concerned gear is clearly more similar to the test gear than to the reference gear. Therefore, if possible, the limiting values should be determined from operating or test experience in which each operating condition (tooth form, material, lubricant, rotational speed, loading, etc.) are as similar as possible to those of the gear in question. In calculating the load capacity or in the calculation of various factors more methods are allowed (see 5.1).

The utilisation of the calculating procedure requires for each case, a realistic estimation of all influential factors, especially the loading, ambient conditions, damage risk (probability of damage) etc. The recommended minimum safety factors must be increased accordingly (see Annex H).

For calculation example, see Annex J.



### Key

X centre distance  
Y relative deviation

$a_1$  centre distance of the concerning gear

$a_T$  centre distance of the standard reference gear (see Table 4)

$a_V$  centre distance of a gear operating or test experiences are available

$\Delta f$  relative deviation between a quantity of the concerning gear and a reference gear

$\Delta f_T$  here used as relative deviation between the centre distance of the concerning gear and the standard reference gear

$\Delta f_V$  here used as relative deviation between the centre distance of the concerning gear and a gear operating or test experiences are available

**Figure 6 — Deviation as a function of the centre (based on linear regression)**

## 5.1 Applicability

The technical information provided in this Technical Report is based on the following:

- on knowledge and judgement acquired over years of experience in designing, manufacturing and operating worm gearing.
- on results of bench testing I form worm gears having centre distances from 65 to 160 mm and transmission ratios for 4,8 to 50.

Three methods are provided for the calculation of each parameter:

- method A (the most accurate derived from experimental and measurement data)
- method B (calculated parameters derived using numerical methods)
- method C (approximated methods)

## 5.2 Validity

The validity for the various parts of the calculating procedure of this standard are restricted to conditions where operating experience already exists. If further test results are available, a calibration of a valid calculation procedure with respect to type and extent of the concerned testing the scope of validity can be extended.



The rating and design procedures are valid for the following:

- **flank forms:** A, N, K, I, C according to ISO/TR 10828
- **worm rotational speed** up to 5000 r/min
- **gear ratio** from 5 to 100
- **sliding velocity** between tooth surfaces up to 25 m/s for wear not below 0,1 m/s
- **shaft angle** of 90°
- **accuracy grade:** the worm accuracy grade (according to DIN 3974) is assumed to be one accuracy grade better than wheel
- **worm materials:**
  - case hardened steels, case hardened (HRC = 58 ... 62);
  - through hardened steels, flame or induction hardened (HRC = 50 ... 56);
  - the calculation procedures are based on experiments carried out with worms made of 16MnCr5 (case hardened), no studies having been carried out for other materials yet. However, in the case of sufficient surface hardness (as above), hardness penetration depth, core hardness, and correct heat treatment, the calculation procedures of the above mentioned materials can be used;
  - other materials and heat treatments [such as nitriding steels, gas nitrided] can be used with sufficient experience in accordance with method A.
- **worm wheel materials:** Material and notes based on experience are as listed in Table 3.
 

NOTE Other materials not listed in Table 3 can be used.
- **centre distance:**
  - for temperature calculation (wear, pitting) the range is from 60 mm up to 500 mm centre distance;
  - for other criteria (pitting, tooth breakage) the range is between 50 mm up to 500 mm centre distance.
- **lubricants:**
  - mild additive CLP-oils according to ISO 6743-6:1990;
  - compounded oils (steam cylinder oils), no test results available, included as a mineral oil in this standard;
  - polyglycols;
  - polyalphaolefines based on limited test results.

The calculations are based essentially on studies carried out with I-worm gears. The results have been converted to worm gears with other flank forms by means of similarity considerations.

Table 3 — Common worm wheel materials

Worm Material	16MnCr5 Case Hardened					
Wheel Material	GZ-CuSn12 <sup>1)3)</sup>	GZ-CuSn12Ni2 <sup>1)</sup>	GC-CuSn12Ni2 <sup>1)</sup>	GZ-CuAl10Ni <sup>1) 2)</sup>	GGG-40	GG-25
Wear	+	+	+	o	o	o
Pitting	+	+	+	o	-	-
Tooth Breakage	+	+	-	+	+	+
Temperature	+	+	+	+	-	-
+: covered study available o: known study -: empirical values <sup>1)</sup> Bronze should be homogenous and free from blow holes in the gearing region. Average grain size < 150 µm. Grain size variation may have a significant influence, on the capacity, resulting in variation of 20% or more, if not maintained consistent. For the determination of grain size minimum of 50 grains are needed to be observed on the area of active flanks. <sup>2)</sup> Forged aluminium bronze can be treated like GZ-CuAl10Ni <sup>3)</sup> Forged phosphor bronze can be treated like GZ-CuSn12						
NOTE 1 See EN 1982, EN 1563 and EN 1561 for the material designation						
NOTE 2 For low sliding velocities, $v_g < 0,5$ m/s.						

### 5.3 System considerations

In this Technical Report no attempt is made to address complete drive systems, backdriving, torsional vibrations, critical speeds or other types of vibrations which may affect operation of worm gears.

### 5.4 Calculation methods A, B, C

This Technical Report contains influential factors based on research results and operational experiences. The factors are differentiated with reference to:

- Factors which are concerned with meshing geometry or compatibility are calculated using given equations.
- Factors which are multi-influenced, or are independent of each other (which do not however affect each other), or both. These include factors which affect an influence on the permitted stress.

The factors can be determined by different methods which are, where necessary, characterised by additional parameters A to C. Method A is more precise than B and so on. It is recommended to use the most precise method. With important operations it is recommended that the method used is agreed upon by manufacturer and purchaser.

#### Method A:

Here the factor is determined through exact measurement, extensive mathematical analysis of the transfer system or existing operational experiences. Because of this, all gear and loading data must be known.

#### Method B:

The factors are determined by a method which, for most applications, is sufficiently precise. The assumptions under which they are developed are stated. In determining a specific factor, the application should be within the range of the given assumptions.

**Method C:**

For some factors additional simplified approximation procedures are specified. The assumptions under which they are developed are stated. In determining a specific factor, the application should be within the range of the given assumptions.

**5.4.1 Notes on numerical equations**

The equations specified in this Technical Report must be calculated in the specified units (see Table 1).

**5.4.2 Base conditions, interaction**

## — Wear:

This procedure is in accordance with the investigation described in Bibliography [24] and is based on practical experience.

## — Pitting damage:

The procedure follows the investigation described in Bibliography [31] and takes into consideration practical experience. The Hertzian stress is an essential influencing variable to the physics causing pitting development, in addition to this however, other influences are also of importance e.g. the tangential forces and the effects of slip and roll movement. According to present day theory however, these need not be considered. For the above reasons the limiting value of the load capacity (surface stress values) should be developed through tests on worm gears or through evaluation of relevant operational results. Allowable values, resulting from specimen examination (e.g. disk tests), only allow for relative statements and may only be used for the load capacity calculation if scientific investigation of this manner has been completed.

## — Interaction between scuffing and wear:

Short term scuffing incurred by bronze wheels can be "healed". This healing is only possible through wear, however estimations of wear life under this condition cannot be considered at the moment.

## — Interaction between wear and pitting:

It is known from practical testing that pitting development can be stabilised by increased wear. Pitting can also be stopped through continual wear.

At higher wear intensities, that is when the wear capacity limits the life endurance, pitting is a secondary consideration. Alternatively with higher pitting, wear is not the limiting criteria.

## — Interaction between wear and tooth breakage:

The calculation of the tooth breakage factor takes into account that the tooth thickness of the worm wheel is decreased by wear.

**5.4.3 Other notes**

Proof of load capacities are provided by continual endurance operation. With implementation procedures, intermittent operation and alternating loading etc. the experience of the gear manufacturer must be considered.

**5.5 Standard reference gear**

With certain calculation procedures the absolute calculating equations are similar to the relative calculating equations. If the adopted sizes of the corresponding standard reference gear (subscript T) must be employed, the relative calculating equations can be transferred to the absolute calculating equations (see Table 4).

Table 4 — Main data from the standard reference gear

Centre distance $a_T$	100 mm
Gear ratio $u_T$	20,5
Worm reference diameter $d_{m1T}$	36 mm
Worm wheel reference diameter $d_{m2T}$	164 mm
Parameter for mean hertzian stress $p_{mT}^*$	0,92 (eq. (53))
Parameter for mean lubricant film thickness $h_T^*$	0,07 (eq. (55))
Parameter for mean sliding path $s_T^*$	30,8 (eq. (59))
Worm material	16MnCr5 case hardened
Wheel material	GZ-CuSn12Ni2
Lubricant density	1,048 kg/dm <sup>3</sup>
Flank form	I
Normal pressure angle	20°
Worm surface roughness $Ra_1$	0,5 µm
Equivalent modulus of elasticity $E_{red}$	150 622 N/mm <sup>2</sup>

## 6 Geometrical data to be known for calculation

### 6.1 Input variables

For the calculation the following variables have to be known:

#### Geometry data:

- Center distance,  $a$
- Face width,  $b_{2H}$ , see Figure 7
- Wheel rim width,  $b_{2R}$ , see Figure 7
- Reference diameter,  $d_{m1}$ ,  $d_{m2}$
- Axial module of the worm,  $m_{x1}$
- Number of teeth,  $z_1$ ,  $z_2$
- Addendum modification factor,  $x_2$
- Pressure angle  $\alpha_1$
- Profile flank form, (A, N, K, I, C)
- Outside diameter,  $d_{e2}$
- Rim thickness,  $s_k$ , see Figure 7
- Worm tip diameter,  $d_{a1}$
- Worm tooth thickness in axial section divided by axial pitch,  $s_{mx1}/p_{x1}$

#### Loading:

- Nominal output torque,  $T_2$
- Application factor,  $K_A$
- Rotational speed of worm,  $n_1$
- Life time,  $L_h$
- Number of start per hour,  $N_S$

Also necessary in order to calculate the efficiency, the power loss and the wear and pitting safety factors:

- Worm and wheel material
- Lubricant data  $\rho_{oil}$ ,  $\nu_{40}$ ,  $\nu_{100}$
- Type of oil: mineral oil / polyglycol
- Type of lubrication: splash or spray lubrication
- Roughness of the worm flanks,  $Ra_1$
- Immersed or not immersed worm wheel
- Type of bearing at the worm: located – non located bearing; adjusted bearing
- Number of sealing rings at the worm
- Housing with fan or housing without fan
- Ambient temperature  $\theta_0$

To calculate the deflection safety factor:

Worm bearing spacing,  $l_1$ , or  $l_{11}$ ,  $l_{12}$

To calculate the tooth root safety factor:

- Accuracy grade of pitch deviation by analogy with DIN 3974
- Tooth rim thickness,  $s_K$
- Throat radius  $r_{g2}$
- Root diameter  $d_{f2}$

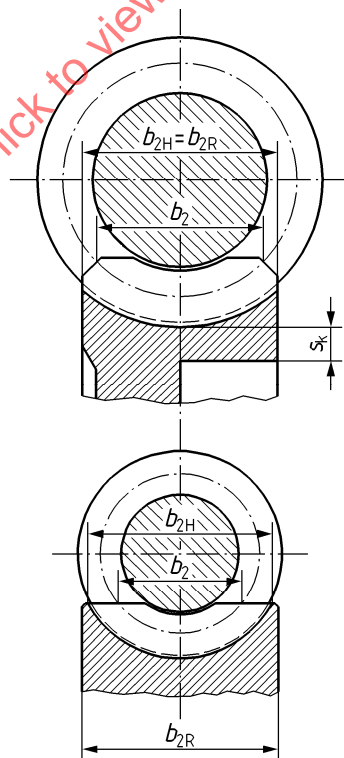


Figure 7 — Wheel tooth and rim thickness

## 6.2 Safety factors

It is of particular importance to the choice of safety factors that the requirements can be considerably varied with differing fields of application. Safety factors (calculated) are differentiated according to wear,  $S_W$ , pitting,  $S_H$ , deflection,  $S_\delta$ , tooth breakage,  $S_F$  and maximum temperature,  $S_T$ . The defined minimum safety values,  $S_W$ ,  $S_H$ ,  $S_\delta$ ,  $S_F$  and  $S_T$  should not be reduced. In this Technical Report numerical values are given for these.

The safety factors should be chosen after careful consideration of the following influences:

- how safe are the assumptions of the concerning load
- how safe are the assumptions of the concerning operating conditions
- what are the consequences of damage.

**It is recommended that the safety factors are agreed upon by manufacturer and purchaser.**

## 7 Forces, speeds and parameters for the calculation of stresses

For the calculation of load capacity, the following forces, speeds and parameters are required, which can be used to describe stress mechanisms of both tooth flank and tooth root which are essential to the damages mentioned above.

When arranging the force application, all forces transferred to the gear must be compiled as accurately as possible. This should also be considered in the calculation. This is particularly important for the reliability and accuracy of the calculation.

### 7.1 Tooth forces

When calculating the tooth forces the external and internal influences must be taken into account (see 7.1.1 and ISO 6336-6).

#### 7.1.1 Application factor

The application factor,  $K_A$ , considers all forces externally introduced to the gear, in addition to the nominal forces described in 7.1.2. These extra forces depend on the driving machine characteristics and driven machine characteristics, the masses and elasticities in the output and drive lines (e.g. from shafts and clutches) and operating conditions. Guide values for  $K_A$  can be found in ISO 6336-6.

#### 7.1.2 Dynamic factor

Internal influences are covered by factor  $K_v$ .

The measurement of the tooth root stresses at different circumferential velocities ( $\omega_2$ ) has indicated that the amount of internally generated dynamic loads can be neglected ( $K_v = 1$ ).

#### 7.1.3 Load distribution factor

Influence of load distribution are covered by factor  $K_{H\beta}$  and  $K_{H\alpha}$ .

The methods within the Technical Report assume that the worm gear has been accurately manufactured and run-in, such that there is a load distribution over the face width (along the contact lines) and with all the sequentially meshed gears ( $K_{H\alpha} = K_{H\beta} = 1$ ).

Variable torque, which results in varying worm deflections, however, may result in non-uniform load distribution along the contact lines with correspondingly increased wear during gear operation. In order to keep this effect to a minimum, a deflection safety factor is required (see Clause 11).

### 7.1.4 Tooth force components

The torques required for the calculations of the following forces are calculated from the nominal input and output torques as follows:

$$T_1 = T_{1N} \cdot K_A \quad (43)$$

$$T_2 = T_{2N} \cdot K_A \quad (44)$$

The basis for the load capacity calculation is the rated torque of the driven machine, that is the operational torque for the heaviest working conditions. The nominal torque can also be taken from the motor provided that this torque corresponds with the permissible torque of the driven machine. If this is not the case another sensible definition should be chosen.

The tangential, axial and radial forces,  $F_{tm1,2}$ ,  $F_{xm1,2}$ ,  $F_{rm1,2}$ , acting on the worm and wheel are shown in Figure 8.

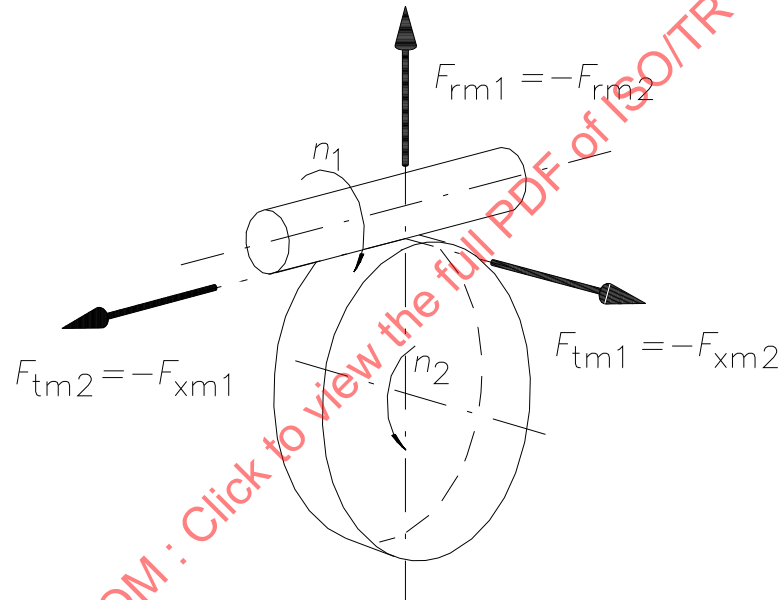


Figure 8 — Tooth load components

**Worm driving the worm wheel:**

$$F_{tm1} = 2000 \cdot \frac{T_1}{d_{m1}} = 2000 \cdot \frac{T_2}{d_{m1} \cdot \eta_{ges} \cdot u} = -F_{xm2} \quad (45)$$

$$F_{tm2} = 2000 \cdot \frac{T_2}{d_{m2}} = 2000 \cdot \frac{T_1 \cdot \eta_{ges} \cdot u}{d_{m2}} = -F_{xm1} \quad (46)$$

with  $\eta_{ges}$  according to Equation (77)

$$F_{rm1} = -F_{rm2} = F_{tm1} \cdot \frac{\tan \alpha_0}{\sin(\gamma_{m1} + \rho_z)} \quad (47)$$

with:  $\rho_z = \arctan(\mu_{zm})$

$\mu_{zm}$  according to Equation (90)

**Worm wheel driving the worm:**

$$F_{tm1} = 2000 \cdot \frac{T_1}{d_{m1}} = 2000 \cdot \frac{T_2 \cdot \eta'_{ges}}{d_{m1} \cdot u} = -F_{xm2} \quad (48)$$

$$F_{tm2} = 2000 \cdot \frac{T_2}{d_{m2}} = 2000 \cdot \frac{T_1 \cdot u}{d_{m2} \cdot \eta'_{ges}} = -F_{xm1} \quad (49)$$

with  $\eta'_{ges}$  according to Equation (78)

$$F_{rm2} = -F_{rm1} = F_{tm2} \cdot \frac{\tan \alpha_0}{\cos(\gamma_{m1} - \rho_z)} \quad (50)$$

**7.2 Sliding velocity at mean reference diameter**

Due to the mostly large slip components in the circumferential direction it is sufficient to use the sliding velocity at the reference diameter  $v_g$  in flank direction, to calculate the load capacity:

$$v_g = \frac{d_{m1} \cdot n_1}{19098 \cdot \cos \gamma_{m1}} \quad (51)$$

**7.3 Physical parameters**

In order to judge the capacity of worm gears, non-dimensional parameters are defined,  $p_m^*$ , for the mean Hertzian stress,  $h^*$ , for the mean lubricant film thickness and  $s^*$ , for the mean sliding path. These parameters are dependant only on the geometry of the used gears. Size, loading and lubricant do not influence them. See Bibliography ([24] and [32]) for description of their derivations.

The parameters are derived according to methods A, B and C.

NOTE 1 The use of method C does not eliminate the need to check that proper gear mesh occurs.

NOTE 2 The approximation of A, I, N, K profiles of worms as a unique profile in the equations given in Method C is only mathematical.

**Method A:**

The physical parameters are directly derived from experimental and measurement data. At present this is not yet possible.

**Method B:**

The physical parameters are derived using numerical methods; see Bibliography ([32] and [36]) (for physical basis of the parameters see 7.1.3 and 7.1.4 and Annexes B, C, D, E and F).

**Method C:**

Solutions for the physical parameters can be obtained through approximation equations from computer - programming according to Bibliography ([21], [32] and [36]).

The equations apply to flank form I but can also be used in an approximate manner for tooth forms K, A and N. The approximation formulae for C-worm drives are derived from Bibliography [25] and from operational experience. The approximation equations indicated in 7.3.1, 7.3.2 and 7.3.3 apply to I-worm drives with  $\alpha_n = 18 \dots 22^\circ$ ,  $x_2 = -0,5 \dots + 1$ ,  $h_{am1} + h_{am2} \approx 2 \cdot m_{x1}$ , C-worm drives with  $\alpha_n = 20 \dots 24^\circ$ ,  $x_2 = 0 \dots + 0,5$ ,  $h_{am1} + h_{am2} \approx 2 \cdot m_{x1}$  and  $\rho/m_n \approx 5 \dots 7$ .



For I – Wormdrive, the approximation equations supplies only sensible results if the base diameter does not lie in the active flanks.

The approximation equations are only valid for a worm wheel facewidth:

$$b_{2H, std} = m_{x1} \left( \sqrt{q_1^2 - (q_1 - 3)^2} + 1 \right) \quad (52)$$

For a smaller worm wheel face width the physical parameters for  $p_m^*$  and  $h^*$  are on the unsafe side. Therefore higher safety factors for wear and pitting have to be used or the physical parameters  $p_m^*$  and  $h^*$  are calculated according Method B.

### 7.3.1 Mean hertzian stress

The mean hertzian stress is a parameter of essential importance to the flank loading (see 5.1.3)

#### a) Parameter for the mean hertzian stress - Method A

A parameter which describes the complex relationships between hertzian stress and flank loading cannot be given at the moment.

#### b) Parameter for the mean hertzian stress - Method B

The mean hertzian stress used for the determination of the parameter is calculated by means of computer programming e.g. according to Bibliography ([21], [32] and [36]) under assumption of the equal hertzian pressure for all simultaneously meshed contact lines. Firstly the contact lines are defined then the curvature radii at the flanks on specific contact line sections. In general, for the flanks which now have been approached by equivalent cylinders along the contact lines, the hertzian stress can be derived. In each meshing zone more than one tooth is engaged. The hertzian contact stress along these contact lines are assumed constant. The mean hertzian stress  $p_{Hm}$ , is thus derived from all hertzian stresses from all the meshing zones.

Further calculation according to 7.4, Equation (61) can, with this hertzian stress, now follow. Also, from this hertzian stress, the development of a non - dimensional parameter,  $p_m^*$ , is possible. This parameter of the hertzian stress is only dependant on the gear tooth geometry and is independent of the E-module, material used and centre distance (size). The parameter  $p_m^*$ , is used in Equation (61) for the derivation of the mean contact stress  $\sigma_{Hm}$  (see Annex B, for details of calculation).

#### c) Parameter for the mean hertzian stress - Method C

From calculations according to method B a useful non - dimensional parameter for the mean hertzian stress,  $p_m^*$  is derived.

For I, N, K, A worm drives:

$$p_m^* = 0,1794 + 0,2389 \cdot \frac{a}{d_{m1}} + 0,0761 \cdot x_2 \cdot |x_2|^{3,18} + 0,0536 \cdot q_1 - 0,00369 \cdot z_2 - 0,01136 \cdot \alpha_n \\ + 44,9814 \cdot \frac{x_2 + 0,005657}{z_2} \cdot \left( \frac{z_1}{q_1} \right)^{2,6872} \quad (53)$$

For C-worm drives:

$$p_m^* = 0,1401 + 0,1866 \cdot \frac{a}{d_{m1}} + 0,0595 \cdot x_2 \cdot |x_2|^{3,18} + 0,0419 \cdot q_1 - 0,00288 \cdot z_2 - 0,0089 \cdot \alpha_n$$

$$+ 35,1417 \cdot \frac{x_2 + 0,005657}{z_2} \cdot \left( \frac{z_1}{q_1} \right)^{2,6872} \quad (54)$$

For worm wheel with smaller facewidth than  $b_{2H, \text{std}}$   $p_m^*$  has to be modified with the following equations:

$$p_m^* = p_m^* \cdot f_p$$

$$f_p = \frac{14 \cdot b_2^2 - (28 \cdot b_{2H, \text{std}} + m_{x1}) \cdot b_2 + 300 \cdot m_{x1}^2 + 14 \cdot b_{2H, \text{std}}^2 + b_{2H, \text{std}} \cdot m_{x1}}{300 \cdot m_{x1}^2} \quad (55)$$

This equation is only valid for  $b_{2H, \text{std}} - 2,5 m_{x1} \leq b_{2H} \leq b_{2H, \text{std}}$ . For smaller value than  $b_{2H, \text{std}} - 2,5 m_{x1}$  Method B has to be used. For higher value than  $b_{2H, \text{std}}$   $f_p = 1$ .

### 7.3.2 Mean lubricant film thickness

The mean lubricant film thickness is a parameter of essential importance to the calculation of the flank load capacity and the efficiency.

#### a) Parameter for the mean lubricant film thickness - Method A

A parameter which describes the complex relationship between changeable lubricant film thickness above the meshing zone and flank loading cannot be given at the moment.

#### b) Parameter for the mean lubricant film thickness - Method B

The mean minimum lubricant film thickness  $h_{\min m}$  is derived by means of computer programming (see Bibliography ([21], [32] and [36])) based on a method from Dowson and Higginson (see Bibliography). The tooth flanks must be replaced in sections along the specific contact lines by means of rolling with the flank curvature. Under consideration of velocity relationships the hertzian stress and the lubricant properties the minimum lubricant film thickness  $h_{\min m}$  for specific roll sections can be calculated using Bibliography [19]. The mean minimum lubricant film thickness can now be given from the mean value of all the minimum lubricant film thicknesses for all contact points. From the minimum mean lubricant film thickness a non dimensional parameter  $h^*$  for the lubricant film thickness is given. This parameter is only dependant on the gearing geometry. It is independent from centre distance (size), velocity, rate of revolutions, lubricant and loading. The relationship between  $h^*$  and  $h_{\min m}$  is shown by Equation (63) (see Annex C, for details of calculation).

#### c) Parameter for the mean lubricant film thickness - Method C

From calculations according to method B a useful non - dimensional parameter for the mean lubricant film thickness,  $h^*$ , is derived.

For I, N, K, A worm drives:

$$h^* = -0,393 + 2,9157 \cdot 10^{-6} \cdot (z_2)^{-0,0847} \cdot \alpha_n^{0,0595} \cdot (7,947 \cdot 10^{-7} \cdot x_2 + 5,927 \cdot 10^{-5}) \cdot ((1 - 0,038 \cdot q_1) \cdot q_1 + 65,576) \cdot$$

$$\left( \left( 108,8547 \cdot \frac{z_1}{q_1} - 1 \right) \cdot \frac{z_1}{q_1} - 3294,921 \right) \cdot (3,291 \cdot 10^{-3} \cdot B + 1) \cdot B - 13064,58 \quad (56)$$

with  $B = \sqrt{6 \cdot m_{x1} \cdot d_{m1} - 9 \cdot (m_{x1})^2} + m_{x1}$

For C-worm drives:

$$h^* = -0,511 + 3,7904 \cdot 10^{-6} \cdot (z_2)^{-0,0847} \cdot \alpha_n^{0,0595} \cdot (7,947 \cdot 10^{-7} \cdot x_2 + 5,927 \cdot 10^{-5}) \cdot ((1 - 0,038 \cdot q_1) \cdot q_1 + 65,576) \cdot \left( \left( 108,8547 \cdot \frac{z_1}{q_1} - 1 \right) \cdot \frac{z_1}{q_1} - 3294,921 \right) \cdot \left( (3,291 \cdot 10^{-3} \cdot B + 1) \cdot B - 13064,58 \right) \quad (57)$$

with  $B = \sqrt{6 \cdot m_{x1} \cdot d_{m1} - 9 \cdot (m_{x1})^2} + m_{x1}$

For worm wheel with smaller facewidth than  $b_{2H, \text{std}}$   $h_m^*$  must to be modified with the following equations:

$$h^* = h^* \cdot f_h$$

$$f_h = \frac{-2 \cdot b_2^2 + (4 \cdot b_{2H, \text{std}} + m_{x1}) \cdot b_2 + 75 \cdot m_{x1}^2 - 2 \cdot b_{2H, \text{std}}^2 - b_{2H, \text{std}} \cdot m_{x1}}{75 \cdot m_{x1}^2} \quad (58)$$

This equations is only valid for  $b_{2H, \text{std}} - 2,5 m_{x1} \leq b_{2H} \leq b_{2H, \text{std}}$ . For smaller value than  $b_{2H, \text{std}} - 2,5 m_{x1}$  Method B must be used. For higher value than  $b_{2H, \text{std}}$   $f_h = 1$ .

### 7.3.3 Mean sliding path

The sliding path of a contact point of the worm flank within the width of hertzian flattening is a parameter of essential importance to the flank load.

#### a) Parameter for the mean sliding path - Method A

A parameter which describes exactly the complex relationship between changeable sliding path above the meshing zone and flank loading cannot be given at the moment.

#### b) Parameter for the mean sliding path - Method B

The sliding path  $s_{gB}$ , is the sliding path of a point of the worm flank within the width of hertzian flattening. On the basis of local  $s_{gB}$  values the arithmetical mean value from all contact lines of the meshing zone is calculated. This is calculated by computer programming (see Bibliography ([21], [32] and [36])).

On this basis a non-dimensional parameter  $s^*$ , is defined for the sliding path (see Annex D, for details of calculation).

#### c) Parameter for the mean sliding path - Method C

From calculations according to method B a useful non-dimensional parameter for the mean sliding path  $s^*$  for common dimensions, is derived.

For I, N, K, A worm drives:

$$s^* = 0,78 + 0,21 \cdot u + 5,6 / \tan \gamma_{m1} \quad (59)$$

for C-worm drives:

$$s^* = 0,94 + 0,25 \cdot u + 6,7 / \tan \gamma_{m1} \quad (60)$$

## 7.4 Calculation of the mean contact stress

Mean contact stress  $\sigma_{Hm}$ , corresponding to 7.3.1

$$\sigma_{Hm} = \frac{4}{\pi} \cdot \left( \frac{p_m^* \cdot T_2 \cdot 10^3 \cdot E_{red}}{a^3} \right)^{0,5} \quad (61)$$

The parameter for mean contact stress  $p_m^*$ , is derived as stipulated in 7.3.1 (method B or C).

Equivalent modulus of elasticity:

$$E_{red} = \frac{2}{(1 - \nu_1^2) / E_1 + (1 - \nu_2^2) / E_2} \quad (62)$$

For different material combinations the modulus of elasticity, POISSON ratio and the equivalent modulus of elasticity  $E_{red}$ , are given in Table 5.

**Table 5 — Modulus of elasticity, and cross sectional contraction parameter for wheel materials**

Wheel material	GZ-CuSn12	GZ-CuSn12Ni2 GC-CuSn12Ni2	GZ-CuAl10Ni	GGG-40	GG-25
$E_2$ [N/mm <sup>2</sup> ]	88 300	98 100	122 600	175 000	98 100
$\nu_2$ [-]	0,35	0,35	0,35	0,3	0,3
$E_{red}$ [N/mm <sup>2</sup> ]	140 114	150 622	174 053	209 790	146 955
NOTE see Bibliography [31], equivalent modulus of elasticity $E_{red}$ , for the combination with a steel worm ( $E_1 = 210000$ N/mm <sup>2</sup> , $\nu_1 = 0,3$ )					

## 7.5 Calculation of the mean lubricant film thickness

With some simplifications (see Annex C and Bibliography [19]), the following applies:

$$h_{min m} = 21 \cdot h^* \cdot \frac{c_\alpha^{0,6} \cdot \eta_{0M}^{0,7} \cdot n_1^{0,7} \cdot a^{1,39} \cdot E_{red}^{0,03}}{T_2^{0,13}} \quad (63)$$

(for units, see in Clause 3)

The parameter for the lubricant film thickness  $h^*$ , must be determined in accordance with 7.3.2 (method B or C).

Here, the mostly unknown pressure viscosity exponent,  $\alpha$ , is replaced by an approximated constant,  $c_\alpha$ , which is a function of the oil type:

— for mineral oils or compounded oils:

$$c_\alpha = 1,7 \cdot 10^{-8} \text{ in } m^2/N \quad (64)$$

— for polyalphaolefines:

$$c_\alpha = 1,4 \cdot 10^{-8} \text{ in } m^2/N \quad (65)$$

— for polyglycols:

$$c_{\alpha} = 1,3 \cdot 10^{-8} \text{ in } \text{m}^2/\text{N} \quad (66)$$

The dynamic viscosity  $\eta_{0M}$ , at ambient pressure  $p_0$ , and wheel bulk temperature  $\theta_M$ :

$$\eta_{0M} = \nu_M \cdot \rho_{oilM} / 1000 \quad (67)$$

The kinematic viscosity  $\nu_M$ , must be determined by Equation (74) or from the viscosity-temperature characteristic line of the lubricant at the wheel bulk temperature  $\theta_M$ , (see Clause 14 for the determination of the wheel bulk temperature  $\theta_M$ ).

The lubricant density  $\rho_{oilM}$ , at the wheel bulk temperature  $\theta_M$ , is (see Bibliography [30]):

$$\rho_{oilM} = \rho_{oil15} / (1 + k \cdot (\theta_M - 15)) \quad (68)$$

Where  $\rho_{oil15}$  is the density of the lubricant at 15 °C (from the data sheet of the oil manufacturer).

Lubricant constant for mineral oils or compounded oils:

$$k = 7,0 \cdot 10^{-4} \quad (69)$$

Lubricant constant for polyalphaolefines:

$$k = 7,6 \cdot 10^{-4} \quad (70)$$

Lubricant constant for polyglycols:

$$k = 7,7 \cdot 10^{-4} \quad (71)$$

## 7.6 Calculation of the wear path

The wear path  $s_{Wm}$  covered is calculated from the number of stress cycles of the wheel  $N_L$  and the sliding path of the worm within the hertzian contact on the wheel flank:

$$s_{Wm} = s_{gm} \cdot N_L = s^* \cdot \frac{\sigma_{Hm} \cdot a}{E_{red}} \cdot N_L \quad (72)$$

The parameter for the mean sliding path,  $s^*$ , must be determined in accordance with 7.3.3 (methods B or C).

Number of stress cycles of the wheel  $N_L$ , for the life expectancy,  $L_h$ :

$$N_L = L_h \cdot \frac{n_1 \cdot 60}{u} \quad (73)$$

## 7.7 Calculation of the lubricant kinematic viscosity

The lubricant kinematic viscosity  $\nu_{\theta}$  for an oil temperature  $\theta$  between 0,1°C and 100°C is calculated from the kinematic viscosity  $\nu_{40}$  at 40°C and the kinematic viscosity  $\nu_{100}$  at 100°C:

$$\nu_{\theta} = 10^{10 \cdot A \cdot \log(\theta + 273) + B} - 0,7 \quad (74)$$

with

$$A = \frac{\log\left(\frac{\log(\nu_{40} + 0,7)}{\log(\nu_{100} + 0,7)}\right)}{\log\left(\frac{313}{373}\right)} \quad (75)$$

$$B = \log(\log(\nu_{40} + 0,7)) - A \cdot \log(313) \quad (76)$$

## 8 Efficiency and power loss

The efficiency or power loss is needed for the calculation of tooth force components and checking of the temperature safety factor.

### 8.1 Total efficiency

#### a) Method A

Determination of the total efficiency from measurements of total power loss at operating conditions at the existing gear.

#### b) Method B

Total efficiency (worm driving wheel):

$$\eta_{ges1-2} = P_2 / (P_2 + P_V) = (P_1 - P_V) / P_1 \quad (77)$$

Total efficiency (wheel driving worm):

$$\eta_{ges2-1} = P_1 / (P_1 + P_V) = (P_2 - P_V) / P_2 \quad (78)$$

The total power loss  $P_V$  shall be derived as is stipulated in 8.2 (method B or C).

### 8.2 Total power loss

#### a) Method A

Measurement of the total power loss at the existing gear.

#### b) Method B

The total power loss  $P_V$ , must be calculated as follows:

$$P_V = P_{Vz} + P_{V0} + P_{VLP} + P_{VD} \quad (79)$$

If the relationship between the meshing power loss and the oil sump temperature is known from previous tests, the meshing power loss  $P_{Vz}$ , can be calculated from the measured oil sump temperature.

The idle running power loss  $P_{V0}$ , cannot, to a satisfactory degree of accuracy, be defined by a simple calculation appropriate to a method B calculation. The dependence on viscosity in particular is the cause of uncertainty. Thus, in general method C is used for the determination of  $P_{V0}$ .

The bearing load power losses  $P_{VLP}$ , can be calculated with calculation procedures from the bearing manufacturer.

The sealing power loss  $P_{VD}$  can be calculated with calculation procedures from the seal manufacturer.

### c) Method C

The total power loss  $P_V$  must be derived from Equation (79). The derivation of the meshing power loss  $P_{VZ}$  is as stipulated in 8.4, the idle running power loss  $P_{VO}$  is as stipulated in 8.2.1, the bearing load power loss  $P_{VLP}$  is as stipulated in 8.2.2 and the sealing power loss  $P_{VD}$  is as stipulated in 8.2.3.

NOTE For more precise calculation on power losses in bearings, seals, it is possible to use ISO/TR 13593.

#### 8.2.1 Idle running power loss

The idle running power loss is (see Bibliography [24]):

$$P_{VO} = 0,89 \cdot 10^{-4} \cdot a \cdot n_1^{4/3} \quad (80)$$

Equation (80) is based on Equation (81):

$$P_{VO} = 0,89 \cdot 10^{-2} \cdot \frac{a}{a_T} \cdot n_1^{4/3} \quad (81)$$

#### 8.2.2 Bearing load power loss

The bearing power loss  $P_{VLP}$ , of a complete gear set due to the bearing load is (see Bibliography [24]):

For adjusted bearing arrangement with defined axial clearance (such as straddle mounted taper roller bearings):

$$P_{VLP} = 0,03 \cdot P_2 \cdot a^{0,44} \cdot \frac{u}{d_{m2}} \quad (82)$$

For located – non-located bearing arrangement:

$$P_{VLP} = 0,013 \cdot P_2 \cdot a^{0,44} \cdot \frac{u}{d_{m2}} \quad (83)$$

Equations (82) and (83) are based on Equations (84) and (85):

For an adjusted bearing arrangement:

$$P_{VLP} = 0,028 \cdot P_2 \cdot \left( \frac{a}{a_T} \right)^{0,44} \cdot \frac{u}{u_T} \cdot \frac{d_{m2T}}{d_{m2}} \quad (84)$$

For a located – non-located bearing arrangement:

$$P_{VLP} = 0,012 \cdot P_2 \cdot \left( \frac{a}{a_T} \right)^{0,44} \cdot \frac{u}{u_T} \cdot \frac{d_{m2T}}{d_{m2}} \quad (85)$$

For a sliding bearing the power loss can be calculated as is stipulated in the relevant literature (see Bibliography [35]).

#### 8.2.3 Sealing power loss

For typical application the following equations can be used.

Power loss per lip:

$$P_{VD} = 11,78 \cdot 10^{-6} \cdot d_{m1}^2 \cdot n_1 \quad (86)$$

Equation (86) is based on Equation (87):

$$P_{VD} = 15,3 \cdot 10^{-3} \cdot \frac{d_{m1}^2}{d_{m1T}^2} \cdot n_1 \quad (87)$$

The power loss at the seals on the worm wheel shaft can be neglected.

#### 8.2.4 Adaptation of the calculation procedure to a specific test

In the case where own measurements of power losses are already available, the above mentioned calculation procedures can be adapted. The values for the standard reference gears in the equations must be replaced by the corresponding test gear values. The constants must be adapted to these measurements.

### 8.3 Gear efficiency

The gear efficiency is needed for the calculation of the meshing power loss, see 8.4.

#### a) Method A

The gear efficiency is derived from the power loss as stipulated in 8.4, method A.

#### b) Method B

Determination of the gear efficiency according to the equations in method C using the total measured total power loss for the corresponding material - lubricant combination in the original housing under operating conditions.

#### c) Method C

Gear efficiency  $\eta_{Z1-2}$  (worm driving the wheel):

$$\eta_{z1-2} = \frac{\tan \gamma_{m1}}{\tan(\gamma_{m1} + \arctan \mu_{zm})} \quad (88)$$

Gear efficiency  $\eta_{Z2-1}$  (wheel driving the worm):

$$\eta_{z2-1} \approx \frac{\tan(\gamma_{m1} - \arctan \mu_{zm})}{\tan \gamma_{m1}} \quad (89)$$

Mean tooth coefficient of friction:

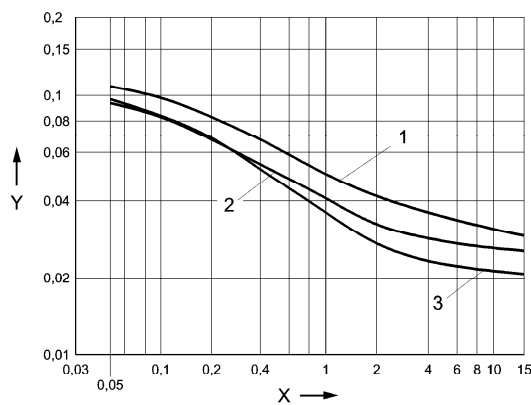
$$\mu_{zm} = \mu_{0T} \cdot Y_S \cdot Y_G \cdot Y_W \cdot Y_R \quad (90)$$

The calculation of the base coefficient of friction  $\mu_{0T}$ , is as stipulated in 8.3.1, the size factor  $Y_S$ , is as stipulated in 8.3.2, the geometry factor  $Y_G$ , is as stipulated in 8.3.3, the material factor  $Y_W$ , is as stipulated in 8.3.4, and the roughness factor  $Y_R$ , is as stipulated in 8.3.5.

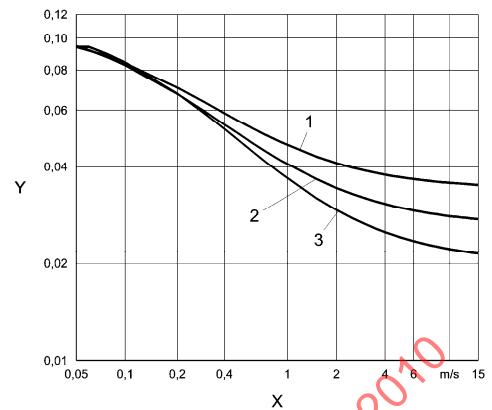
#### 8.3.1 Base coefficient of friction $\mu_{0T}$ , of the standard reference gear

The base coefficient of friction  $\mu_{0T}$ , is a function of the oil type. It can be taken from Figure 9 or derived by the following formulae:

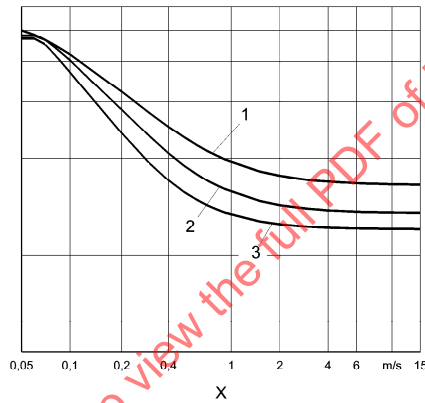




a) Bronze wheels with spray lubrication



b) Bronze wheels with dip lubrication



c) Wheels made of grey cast iron

**Key**

- X mean sliding velocity  $v_g$   
Y basic coefficient of friction  $\mu_{0T}$   
1 lubrication with mineral oil  
2 lubrication with polyalphaolefin  
3 lubrication with polyglycol

**Figure 9 — Base coefficient of friction  $\mu_{0T}$ , of the standard reference gear**

**For bronze wheels, spray lubrication with mineral oil:**

$$\mu_{0T} = 0,028 + 0,026 \cdot \frac{1}{(v_g + 0,17)^{0,76}} \leq 0,1 \quad (91)$$

**For bronze wheels, spray lubrication with polyalphaolefin:**

$$\mu_{0T} = 0,026 + 0,017 \cdot \frac{1}{(v_g + 0,17)^{0,92}} \leq 0,096 \quad (92)$$

**For bronze wheels, spray lubrication with polyglycol:**

$$\mu_{0T} = 0,02 + 0,02 \cdot \frac{1}{(v_g + 0,2)^{0,97}} \leq 0,094 \quad (93)$$

**For bronze wheels, dip lubrication with mineral oil:**

$$\mu_{0T} = 0,033 + 0,079 \cdot \frac{1}{(v_g + 0,2)^{1,55}} \leq 0,1 \quad (94)$$

**For bronze wheels, dip lubrication with polyalphaolefin:**

$$\mu_{0T} = 0,027 + 0,0056 \cdot \frac{1}{(v_g + 0,15)^{1,63}} \leq 0,096 \quad (95)$$

**For bronze wheels, dip lubrication with polyglycol:**

$$\mu_{0T} = 0,024 + 0,0032 \cdot \frac{1}{(v_g + 0,1)^{1,71}} \leq 0,094 \quad (96)$$

**For grey cast iron wheels, lubrication with mineral oil or polyalphaolefin:**

$$\mu_{0T} = 0,055 + 0,015 \cdot \frac{1}{(v_g + 0,2)^{0,87}} \leq 0,1 \quad (97)$$

**For grey cast iron wheels, lubrication with polyglycol:**

$$\mu_{0T} = 0,034 + 0,015 \cdot \frac{1}{(v_g + 0,19)^{0,97}} \leq 0,1 \quad (98)$$

with  $v_g$  according to Equation (51)

### 8.3.2 Size factor

The size factor (see Bibliography [24]) takes into account the influence of centre distance:

$$Y_S = (100/a)^{0,5} \quad (99)$$

Equation (99) is based on the Equation (100):

$$Y_S = (a - 1a)^{0,5} \quad (100)$$

In Equations (99) and (100) if  $a < 65$  mm then  $a = 65$  mm or, if  $a > 250$  mm then  $a = 250$  mm.

### 8.3.3 Geometry factor

The geometry factor (see Bibliography [24]) takes in to account the influence of the gear geometry to the lubricant film thickness:

$$Y_G = (0,07/h^*)^{0,5} \quad (101)$$

with  $h^*$  according to 7.3.2

Equation (101) is based on Equation (102):

$$Y_G = (h_T^* / h^*)^{0,5} \quad (102)$$

### 8.3.4 Material factor

The material factor (see Bibliography [31]) takes into account the influence of the wheel material (Table 6):

**Table 6 — Material factor  $Y_W$**

Wheel Material	GZ-CuSn12	GZ-CuSn12Ni2 GC-CuSn12Ni2	GZ-CuAl10Ni	GGG-40	GG-25
Factor $Y_W$	1,0	0,95	1,1	1,0	1,05

### 8.3.5 Roughness factor

The roughness factor (see Bibliography [34]), takes in to account the influence of the surface roughness of the worm flanks:

$$Y_R = \sqrt[4]{\frac{Ra_1}{0,5}} \quad (103)$$

Equation (103) is based on Equation (104):

$$Y_R = \sqrt[4]{\frac{Ra_1}{Ra_T}} \quad (104)$$

In case the arithmetic mean roughness,  $Ra_1$ , of the worm is not known but the mean roughness depth,  $Rz_1$ , is, a valid approximation is  $Ra_1 = Rz_1 / 6$ .

NOTE The roughness of worm is measured in radial direction of the worm, near the mean cylinder ( $d_{m1}$ ), according to ISO/TR 10064-4.

### 8.3.6 Adaptation of the calculation procedure to a specific test

In the case where some of the coefficients of friction are already available (see Bibliography [29]), the above mentioned calculation procedures can be adapted. The values given in for the coefficients of friction  $\mu_{0T}$ , are replaced by the corresponding derived test friction coefficients. The geometry factor, size factor and roughness factor are now valid for the relationship of the practical test gear (subscript T).

## 8.4 Meshing power loss

### a) Method A

This method is based on the direct measurement of power loss or calculations using coefficient of friction also measured (see Bibliography [29]).

### b) Method B

Determination of the meshing power loss from the measured total power loss for the corresponding material - lubricant combinations in the original housing under operating conditions minus the losses as derived in 8.3.

### c) Method C

Derivation from the gear efficiency. Meshing power loss  $P_{Vz1-2}$ , with the worm driving the worm wheel:

$$P_{Vz1-2} \approx \frac{0,1 \cdot T_2 \cdot n_1}{u} \cdot \left( \frac{1}{\eta_{z1-2}} - 1 \right) \quad (105)$$

with  $\eta_{z1-2}$  according to Equation (88).

Meshing power loss  $P_{Vz2-1}$ , with the wheel driving the worm:

$$P_{Vz2-1} \approx \frac{0,1 \cdot T_2 \cdot n_1}{u} \cdot \left( \frac{1}{\eta_{z2-1}} - 1 \right) \quad (106)$$

with  $\eta_{z2-1}$  according to Equation (89).

## 9 Wear load capacity

Through wear, i.e. continual mass loss, the tooth thickness is decreased. With increasing wear the danger of one of the safety limits stated in 9.3 being violated also increases. In most danger is the lowest flank hardness, mainly the wheel flanks.

### 9.1 Wear safety factor

The following method assumes that full contact pattern is established. Wear load capacity method is independent of the pitting capacity without consideration of any correlation.

The safety against wear is defined as follows:

$$S_W = \delta_{W \lim n} / \delta_{Wn} \geq S_{W \min} \quad (107)$$

The limiting flank loss  $\delta_{W \min}$ , is specified in 9.3, the expected wear (flank loss in normal  $\delta_{Wn}$ ) is defined as in 9.2.

Minimum safety factor:

$$S_{W \min} = 1,1 \quad (108)$$

It may be necessary for C worm drives to use a higher minimum safety factor.

### 9.2 Expected wear

#### 9.2.1 Method A

A more accurate calculation is based on direct measurements of gear sets under operating conditions and a realistic, more accurate analysis of the wear process.

#### 9.2.2 Methods B, C

In calculating the flank loss  $\delta_{Wn}$ , the physical parameters  $p_m^*$ ,  $h^*$  and  $s^*$  are required. Calculation of the parameters as stipulated in 7.3.1 ( $p_m^*$ ), 7.3.2 ( $h^*$ ) and 7.3.3 ( $s^*$ ).

The following procedure describing the derivation of  $\delta_{Wn}$  is based on extensive tests (see Bibliography [24]). In principle only the supplied material - lubricant combinations are calculable ones. For those combinations not given, the procedure can only provide a large approximation. Also if the specification is covered by tests a scatter factor of 2 is normal for the wear speed of the running in gears. Further notes as to the usage of this procedure can be found in Annex E.

Flank loss due to wear  $\delta_{Wn}$  to the wheel flank in normal:

$$\delta_{Wn} = J_W \cdot s_{Wm} \quad (109)$$

The wear path  $s_{Wm}$ , is given by Equations (72) to (73) and Equation (110) gives the wear intensity  $J_W$ . The material – lubricant factor,  $W_{ML}$ , is given in Table 7 and takes into account the influence of the combined effects of the wheel material and lubricant to the wear behaviour (see Bibliography [27] and [28]).

Wear intensity,  $J_W$ :

$$J_W = J_{OT} \cdot W_{ML} \cdot W_{NS} \quad (110)$$

The reference wear intensity,  $J_{OT}$ , is given in or derived by Equation (111) to (121) (see Figure 10).

Linear regression line for bronze wheels with mineral oil:

$$J_{OT} = 2,4 \cdot 10^{-11} \cdot K_W^{-3,1} \leq 400 \cdot 10^{-9} \quad (111)$$

Linear regression line for bronze wheels with polyalphaolefines:

$$J_{OT} = 318 \cdot 10^{-12} \cdot K_W^{-2,24} \quad (112)$$

Linear regression line for bronze wheels with polyglycol:

$$J_{OT} = 127 \cdot 10^{-12} \cdot K_W^{-2,24} \quad (113)$$

Linear regression line for bronze wheels, dip lubrication with mineral oil:

$$J_{OT} = 6,5 \cdot 10^{-11} \cdot K_W^{-2,68} \leq 400 \cdot 10^{-9} \quad (114)$$

Linear regression line for bronze wheels, dip lubrication with polyalphaolefin:

$$J_{OT} = 558 \cdot 10^{-12} \cdot K_W^{-1,91} \quad (115)$$

Linear regression line for bronze wheels, dip lubrication with polyglycol:

$$J_{OT} = 223 \cdot 10^{-12} \cdot K_W^{-1,91} \quad (116)$$

Linear regression line for aluminium bronze wheels, lubrication with mineral oil:

$$J_{OT} = 5,45 \cdot 10^{-9} \cdot K_W^{-1,23} \leq 400 \cdot 10^{-9} \quad (117)$$

Linear regression line for aluminium bronze wheels, lubrication with polyalphaolefin:

$$J_{OT} = 16,6 \cdot 10^{-9} \cdot K_W^{-1,17} \quad (118)$$

Linear regression line for grey cast iron wheels, lubrication with mineral oil:

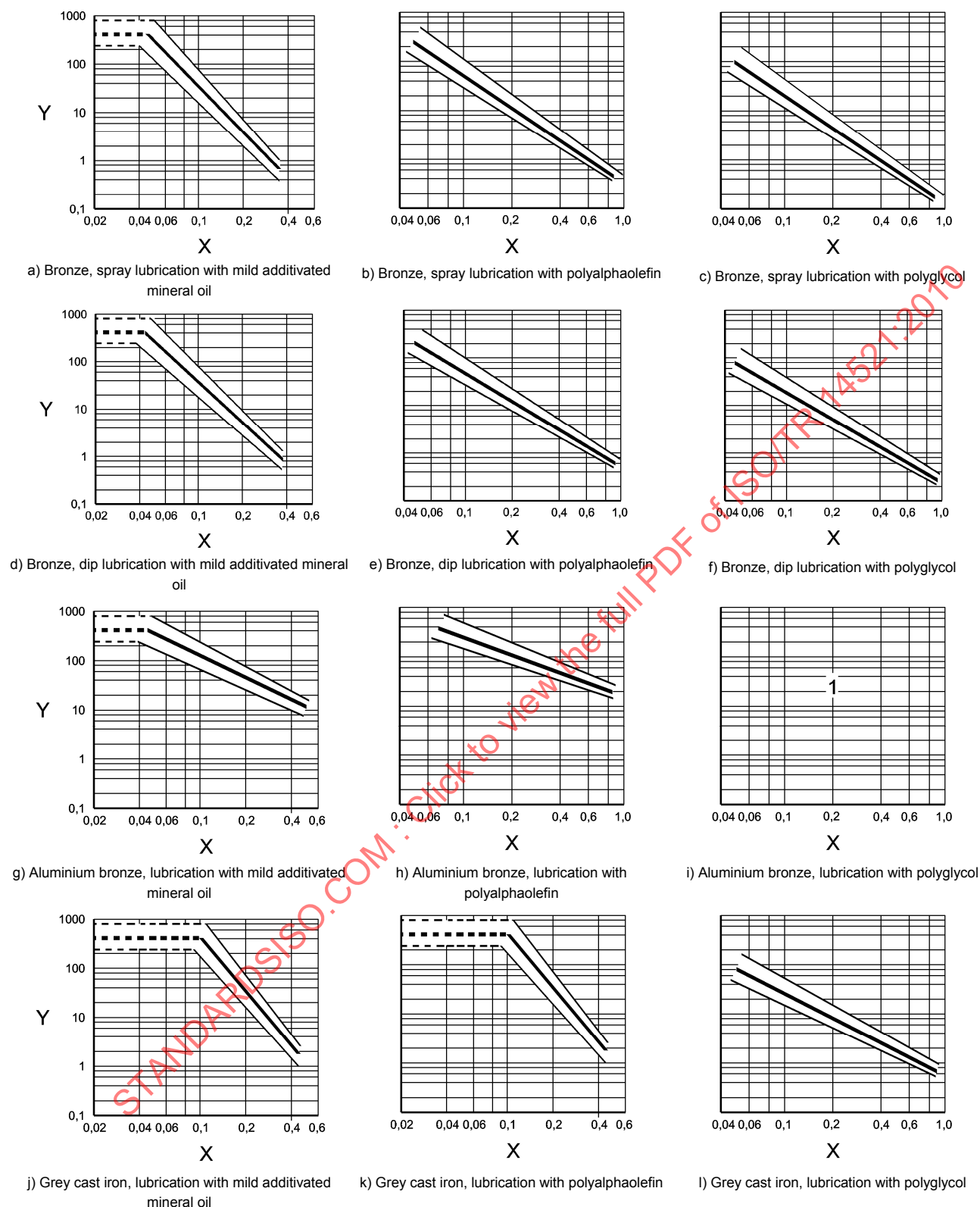
$$J_{OT} = 0,09 \cdot 10^{-9} \cdot K_W^{-3,7} \leq 400 \cdot 10^{-9} \quad (119)$$

Linear regression line for grey cast iron wheels, lubrication with polyalphaolefin:

$$J_{OT} = 0,09 \cdot 10^{-9} \cdot K_W^{-3,7} \leq 400 \cdot 10^{-9} \quad (120)$$

Linear regression line for grey cast iron wheels, lubrication with polyglycol:

$$J_{OT} = 0,58 \cdot 10^{-9} \cdot K_W^{-1,58} \quad (121)$$



### Key

- X film thickness parameter  $K_W$
- Y basic wear intensity  $J_{OT}$  in  $\frac{\text{mm wear}}{\text{mm path}}$
- 1 no data available for the moment

Figure 10 — Basic wear intensity for wheel

Parameter  $K_W$ :

$$K_W = h_{\min m} \cdot W_S \cdot W_H \quad (122)$$

The mean lubricant film thickness  $h_{\min m}$ , is calculated using Equation (63).

For mineral oil, experiments result in a lubricant structure factor of:

$$W_S = 1 \quad (123)$$

For polyglycol and polyalphaolefines:

$$W_S = \frac{1}{\eta_{0M}^{0,35}} \quad (124)$$

The dynamic viscosity  $\eta_{0M}$  (Equation (67)) is taken at ambient pressure,  $p_0$ , and wheel bulk temperature,  $\theta_M$ . The calculation of  $h_{\min m}$  requires the wheel bulk temperature see 13.3.

As the lubricant film thickness and the lubricant structure factor  $W_S$ , are strongly influenced by the wheel bulk temperature, the latter must be calculated by a method which is as sophisticated as possible (see 13.3).

The following notes must be observed:

If other materials or lubricants are used tests should be run, if possible, in order to estimate the effects. The results of any calculations in compliance with this standard can only be taken as a guide.

**Table 7 — Material / lubricant factor  $W_{ML}$**

Worm: 16MnCr5 Case Hardened	Material - Lubricant Factor $W_{ML}$		
	Mineral Oil	Polyalphaolefine PAO	Polyglycol
GZ-CuSn12Ni2	1,0 <sup>a</sup>	1 <sup>a</sup>	1,75 <sup>b</sup>
GC-CuSn12Ni2	4,1	4, 1	4,1
GZ-CuSn12	1,6 <sup>a</sup>	1,6 <sup>a</sup>	2,25 <sup>a</sup>
GZ-CuAl10Ni	1,0 <sup>c</sup>	1,0	— <sup>d</sup>
GGG 40	1,0 <sup>a</sup>	1,0 <sup>a</sup>	1,0 <sup>a</sup>
GG 25	1,0 <sup>a</sup>	1,0 <sup>a</sup>	1,0 <sup>a</sup>
<sup>a</sup> scatter zone $\pm 25\%$ <sup>b</sup> scatter zone $\pm 30\%$ <sup>c</sup> only valid for $h_{\min m} < 0,07 \mu\text{m}$ ; for $h_{\min m} \geq 0,07 \mu\text{m}$ ; $J_W \cong \text{const.} = 600 \cdot 10^{-9}$ . <sup>d</sup> No values are available and risk of scuffing exist. Can be used only for low sliding velocity less than 0,5 m/s and request method A			

The start factor  $W_{NS}$  takes into account the influence of the number of starts per hour,  $N_S$ , on the wear rate (see Bibliography [26]):

$$W_{NS} = 1 + 0,015 \cdot N_S \quad (125)$$

The pressure factor  $W_H$  is according to Reference[29] for bronze materials:

$$W_H = 1 \quad \text{for } \sigma_{Hm} < 450 \text{ N/mm}^2$$

$$W_H = \left( \frac{450}{\sigma_{Hm}} \right)^{4,5} \quad \text{for } \sigma_{Hm} \geq 450 \text{ N/mm}^2 \quad (126)$$

The pressure factor  $W_H$  is according to Reference [26] for grey cast iron materials:

$$W_H = \left( \frac{300}{\sigma_{Hm}} \right)^{1,4} \quad (127)$$

### 9.3 Permissible wear

The permissible wear must be set in accordance with differing criteria a) to d). Criteria a) and b) state a limiting value of flank loss,  $\delta_{W \text{ lim}}$ , which under no circumstances shall be exceeded as this leads to tooth failure. In criteria a) the wear leads to a pointed wheel tooth head, and further wear leads to decreased tooth height. From here the wear increases impropotionally. In criteria b) the wear leads to a weakening of the tooth and eventually to tooth breakage. In criteria c) and d) a restriction of wear is required as opposed to criteria a) and b).

- a) The thickness in the normal section on the outside diameter of the wheel teeth is in no case permitted to become pointed. This provides the limiting value for the permissible wear. The maximum limiting value,  $\delta_{W \text{ lim}}$ , for wear in the normal is therefore as large as the tooth thickness at the tip diameter in the normal.

Tooth thickness at the reference diameter of the wheel is sufficient when calculating the tooth thickness at the outside diameter. The permissible loss in the normal is provided by the usual tooth height  $h_{a1} = m_{x1}$

$$\delta_{W \text{ lim n}} = m_{x1} \cdot \cos \gamma_{m1} \cdot \left( \frac{\pi}{2} - 2 \cdot \tan \alpha_0 \right) \quad (128)$$

- b) The tooth breakage safety factor,  $S_{F \text{ min}}$ , can be attained as the wear condition after the required running time. To this end the following is valid:

$$\delta_{W \text{ lim n}} = \Delta s_{\text{lim}} \cdot \cos \gamma_{m1} \quad (129)$$

The  $\Delta s_{\text{lim}}$  is the allowable tooth thickness loss.

For the tooth thickness loss in the axis,  $\Delta s_{\text{lim}}$ , the same value as in Equation (153) should be taken.

- c) The material loss,  $\Delta m_{\text{lim}}$ , should not exceed a pre-set limit (dependant on oil change intervals and bearing lubrication):

$$\delta_{W \text{ lim n}} = \frac{\Delta m_{\text{lim}}}{A_{fl} \cdot \rho_{\text{Rad}}} \quad (130)$$



with total tooth flank surface  $A_{fl}$ :

$$A_{fl} \approx \frac{z_2 \cdot 2m_{x1} \cdot d_{m1} \cdot \arcsin(b_{2H} / d_{a1})}{\cos \gamma_{m1} \cdot \cos \alpha_0} \quad (131)$$

Wheel material density,  $\rho_{Rad}$ , as shown in Table 8. See Bibliography [31].

**Table 8 — Wheel material density**

Wheel material	GZ-CuSn12	GZ-CuSn12Ni2 GC-CuSn12Ni2	GZ-CuAl10Ni	GGG-40	GG-25
$\rho_{Rad}$ [mg/mm <sup>3</sup> ]	8,8	8,8	7,4	7,0	7,0

- d) The tooth flank loss of the wheel reaches a pre-set value indicated by the backlash. Frequently  $\delta_{Wlim} \equiv 0,3 \cdot m_{x1}$  is applied.

$$\delta_{Wlimn} = 0,3 \cdot m_{x1} \cdot \cos \gamma_{m1} \quad (132)$$

#### 9.4 Adaptation of the calculation procedure to a specific test

The relationships described by Equations (112), (113) or Figure 6 for wear intensity were derived by tests with the standard reference gear and can be checked by tests with other gears. If an application approaching test results is available, the calculation procedure can be calibrated by the relationship between  $J_{OT}$  and the parameter  $K_W = h_{min,m} \times W_S$ . The test conditions should be as similar as possible to the operating conditions of the application, for instance the gear ratio, size etc. of the test gears should be as close to the corresponding values of the concerned application.

If the flank loss through wear,  $\delta_{Wn}$ , of a specific test is known, the basic wear intensity,  $J_{OT}$ , can be derived from Equations (109) and (110). From Equation (112) or (113) a constant can be determined (e.g.  $2,4 \cdot 10^{-11}$  for Equation (112)) which is probably more accurate for the concerned application than the constant in Equation (112).

### 10 Surface durability (pitting resistance)

The tooth flanks can be damaged and eventually destroyed as a consequence of pitting. In most danger are the flanks of lesser hardness, i.e. the wheel flanks.

Pitting can result in the occurrence of wear.

#### 10.1 Pitting safety factor

Pitting safety factor is defined as follows:

$$S_H = \sigma_{HG} / \sigma_{Hm} \geq S_{Hmin} \quad (133)$$

The mean actual contact stress,  $\sigma_{Hm}$ , is defined as is stipulated in 10.2, the limiting contact stress  $\sigma_{HG}$ , is defined as in 10.3.

Minimum safety factor:

$$S_{Hmin} = 1,0 \quad (134)$$

It may be necessary for C worm drives to use a higher minimum safety factor.

The safety factor concerning the transferable torque is equal to the square of  $S_H$  (e.g. if  $S_H = 1,5$  the torque safety is 2,25).

## 10.2 Actual contact stress

### 10.2.1 Method A

The exact calculation of a determinant contact stress is not possible at the moment.

### 10.2.2 Methods B and C

The mean contact stress  $\sigma_{Hm}$ , is used as a load parameter. It is calculated using Equation (61) and the parameter for the mean hertzian stress  $p_m^*$ , as is stipulated in 7.3.1 method B or C.

## 10.3 Limiting value of contact stress

**Limiting value for the contact stress:**

$$\sigma_{HG} = \sigma_{HlimT} \cdot Z_h \cdot Z_v \cdot Z_s \cdot Z_u \cdot Z_{oil} \quad (135)$$

Pitting resistance for contact stress,  $\sigma_{HlimT}$ , are given in Table 9. See Bibliography [31].

**Table 9 — Pitting resistance for contact stress**

Wheel Material	GZ-CuSn12	GZ-CuSn12Ni2 GC-CuSn12Ni2	GZ-CuAl10Ni	GGG-40	GG-25
$\sigma_{HlimT}$ [N/mm <sup>2</sup> ]	425	520	660 <sup>1)</sup>	490 <sup>1)</sup>	350 <sup>1)</sup>
<sup>1)</sup> for low sliding velocities, $v_g < 0,5$ m/s					
NOTE The given endurance limits for contact stress are valid for pitting areas accounting for approx. 50 % of the wheel tooth flank					

**Life factor:**

$$Z_h = (25000 / L_h)^{1/6} \leq 1,6 \quad (136)$$

The life time,  $L_h$ , shall be applied in hours.

**Velocity factor:**

$$Z_v = \sqrt{\frac{5}{4 + v_g}} \quad (137)$$

The sliding velocity at the reference diameter must be determined from Equation (51).

**Size factor:**

$$Z_s = \sqrt{\frac{3000}{2900 + a}} \quad (138)$$

Equation (138) is based on Equation (139):

$$Z_s = \sqrt{\frac{30}{29 + a/a_T}} \quad (139)$$

**Gear ratio factor:**

$$Z_u = \left( \frac{u}{20,5} \right)^{\frac{1}{6}} \text{ for } u < 20,5 \quad (140)$$

$$Z_u = 1 \text{ for } u \geq 20,5$$

Equation (140) is based on Equation (141):

$$Z_u = \left( \frac{u}{u_T} \right)^{\frac{1}{6}} \text{ for } u < 20,5 \quad (141)$$

$$Z_u = 1 \text{ for } u \geq 20,5$$

**Lubricant factor:**

$$Z_{oil} = 1,0 \quad \text{for polyglycols} \quad (142)$$

$$Z_{oil} = 0,94 \quad \text{for polyalphaolefines}$$

$$Z_{oil} = 0,89 \quad \text{for mineral oils}$$

**10.4 Adaptation of the calculation procedure to a specific test**

If test results are available which approach the endurance limits for contact stress the above calculation procedures can be modified as follows. The given values for contact stress endurance limits  $\sigma_{H \lim T}$  must be replaced by the pitting area parameters derived from operational tests. The size factor and transmission factor are thus valid for the behaviour of the practical test gear (subscript T).

**11 Deflection**

Too high and especially continuously changing deflections of the worm shaft result in meshing interferences which again can lead to increased wear.

**11.1 Deflection safety factor**

The deflection safety factor is defined as follows:

$$S_{\delta} = \delta_{\lim} / \delta_m \geq S_{\delta \min} \quad (143)$$

The limiting value for deflection  $\delta_{\lim}$ , is defined as stipulated in 11.3, the actual deflection  $\delta_m$ , is defined as in 11.2.

Minimum safety factor:

$$S_{\delta \min} = 1,0 \quad (144)$$

The safety factor concerning torque is equal to the deflection safety factor  $S_{\delta}$ .

## 11.2 Actual deflection

### 11.2.1 Method A

Measurement of the deflection of the worm shaft in the housing with the used bearing.

### 11.2.2 Method B

More accurate calculation of the deflection of the worm shaft, such as taking account of the centring effect of taper roller bearings, by means of detailed analysis e.g. finite element methods.

### 11.2.3 Method C

Incurred deflection of the worm:

$$\delta_m = 3,2 \cdot 10^{-5} \cdot l_{11}^2 \cdot l_{12}^2 \cdot F_{tm2} \frac{\sqrt{\tan^2(\gamma_{m1} + \arctan \mu_{zm}) + \tan^2 \alpha_0 / \cos^2 \gamma_{m1}}}{d_{m1}^4 \cdot l_1} \quad (145)$$

The bearing spacing  $l_1$ ,  $l_{11}$  and  $l_{12}$  are shown in Figure 11:

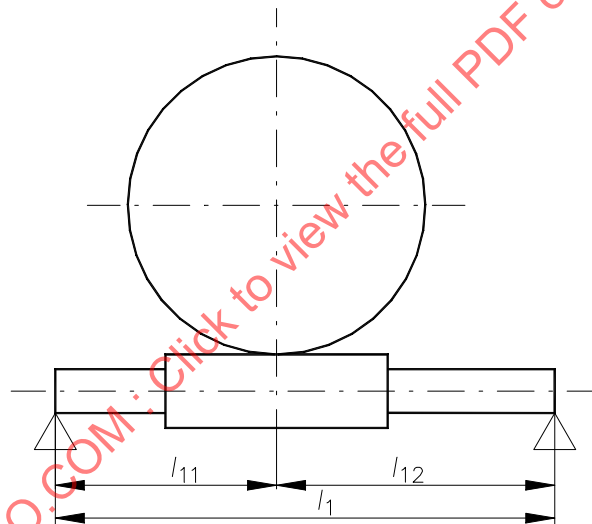


Figure 11 — Bearing spacing

For symmetrical bearing spacing ( $l_{11} = l_{12}$ ) the resultant deflection can be estimated (see Bibliography [31]):

$$\delta_m = 2 \cdot 10^{-6} \cdot l_1^3 \cdot F_{tm2} \frac{\sqrt{\tan^2(\gamma_{m1} + \arctan \mu_{zm}) + \tan^2 \alpha_0 / \cos^2 \gamma_{m1}}}{d_{m1}^4} \quad (146)$$

NOTE Equations (145) and (146) takes only into account the loads due to the gear mesh on the worm shaft. If additional loadings (due to pulley, etc.) are present on the worm shaft these need to be added.

## 11.3 Limiting value of deflection

In accordance with operating experience the limiting value of deflection is:

$$\delta_{lim} = 0,04 \sqrt{m_{x1}} \quad (147)$$

## 12 Tooth root strength

The worm wheel teeth can be plastically deformed or broken as a result of a too high tooth root stress.

### 12.1 Safety factor for tooth breakage

The safety factor for fatigue breakage's is defined as follows:

$$S_F = \tau_{FG} / \tau_F \geq S_{Fmin} \quad (148)$$

The nominal shear stress  $\tau_F$ , is determined as stipulated in 12.2, the limiting nominal shear stress  $\tau_{FG}$ , as in 12.3.

Minimum safety factor:

$$S_{Fmin} = 1,1 \quad (149)$$

The safety factor concerning the transferable torque is equal to that concerning fatigue breakage  $S_F$ .

### 12.2 Actual tooth root stress

#### 12.2.1 Method A

Determination of the tooth root stress through direct measurement of the stresses in the tooth with the aid of strain gauges.

#### 12.2.2 Method B

Determination of the tooth root stress by calculation in accordance with finite element methods.

#### 12.2.3 Method C

The calculation method is based on a nominal shear stress assumption, see Bibliography [23]. The tooth form factor  $Y_F$ , takes into account the bending stress component.

Nominal shear stress at the tooth root  $\tau_F$ :

$$\tau_F = \frac{F_{t2}}{b_{2H} \cdot m_{x1}} \cdot Y_\epsilon \cdot Y_F \cdot Y_Y \cdot Y_K \quad (150)$$

The contact factor  $Y_\epsilon$ , takes into account the load distribution to all simultaneously meshed teeth and is calculated via Equation (151).

The form factor  $Y_F$ , is calculated according to Equation (152), the lead factor  $Y_Y$ , according to Equation (154) and the rim thickness factor  $Y_K$ , according to Equation (155).

$$Y_\epsilon = 0,5 \quad (151)$$

The form factor,  $Y_F$ , takes into account the load distribution over the face width, especially the excess load in the region of the wheel face sides and the load increase due to wear at the tooth roots.

$$Y_F = 2,9 \cdot m_{x1} / s_{ft2} \quad (152)$$

Mean tooth root thickness of the wheel tooth in the transverse is determined without backlash:

$$s_{ft2} = 1,06 \cdot s_{f2} \quad (153)$$

with:  $s_{f2} = s_{m2} - \Delta s_{lim} + (d_{m2} - d_{f2}) \cdot \tan \alpha_0 / \cos \gamma_{m1}$

with:  $s_{m2} \approx p_{x1} \cdot \left(1 - s_{mx1}^*\right)$

$\Delta s$  is the tooth root thickness loss through wear during the required life expectancy.

The lead factor,  $Y_\gamma$ , takes into account the influence of the lead angle and the pertinent excess load at the outlet zone which is also present at run-in gear.

$$Y_\gamma = 1 / \cos \gamma_{m1} \quad (154)$$

The rim thickness factor,  $Y_K$ , takes into account the influence of the rim thickness  $s_K$ , (see Figure 12 for rim thickness),  $\tau_F$ :

$$Y_K = 1,0 \quad \text{for } s_K / m_{x1} \geq 2,0 \quad (155)$$

$$Y_K = 1,043 \ln \left( 5,218 \cdot \frac{m_x}{s_K} \right) \quad \text{for } 1,0 \leq s_K / m_{x1} < 2,0$$

Cases in which  $s_K$  is less than  $1 \cdot m_{x1}$  must be avoided.

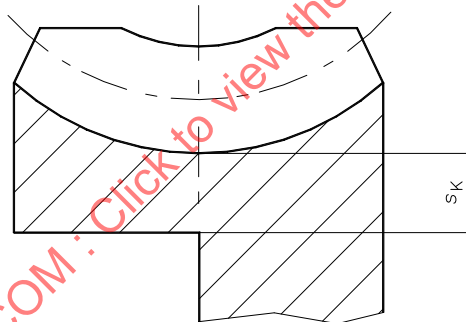


Figure 12 — Rim thickness  $s_K$ , of worm wheel, used to determine the values of  $Y_K$

### 12.3 Limiting value of shear stress at tooth root

Limiting value of shear stress at tooth root:

$$\tau_{FG} = \tau_{F \lim T} \cdot Y_{NL} \quad (156)$$

Shear stress endurance limit  $\tau_{F \lim T}$ , is derived as specified in 12.3.1 and the life factor  $Y_{NL}$ , as in 12.3.2 which takes account of increased load capacity with respect to creep. Here higher plastic deformations can be expected due to permissible accuracy grade deterioration.

#### 12.3.1 Shear endurance limit $\tau_{F \lim T}$

The mean strength endurance values are shown in Table 10. For bronzes, good structures as specified in Clause 1 are assumed. Also, in the field of endurance limits, bronze materials show small plastic deformations. Therefore the reduced value, as shown in Table 10 must be used when an accuracy grade deterioration is not accepted. See Annex F.

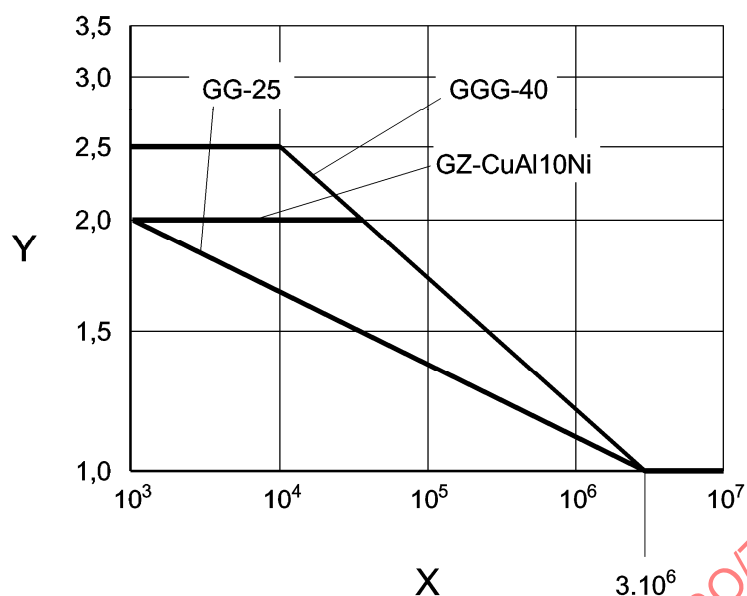
**Table 10 — Mean endurance limits  $\tau_{F \text{ lim } T}$ , for various worm wheel materials**

Wheel Material	GZ-CuSn12	GZ-CuSn12Ni2 GC-CuSn12Ni2	GZ-CuAl10Ni	GGG-40	GG-25
Shear Endurance Limit, $\tau_{F \text{ lim } T}$	92	100	128	115	70
Equivalent Shear Endurance Limit, $\tau_{F \text{ lim } T}$	82	90	120	115	70

**12.3.2 Life factor  $Y_{NL}$** 

For worm wheels of initial accuracy grade up to 7, the life factor  $Y_{NL}$ , as a function of wheel material and the permissible accuracy grade deterioration can be taken from Figure 13 or calculated using the equations shown in Table 11. Plastic deformation leads to a decrease in the gear wheel accuracy grade. The manufacturer experience must be considered for wheel qualities better than accuracy grade 7.

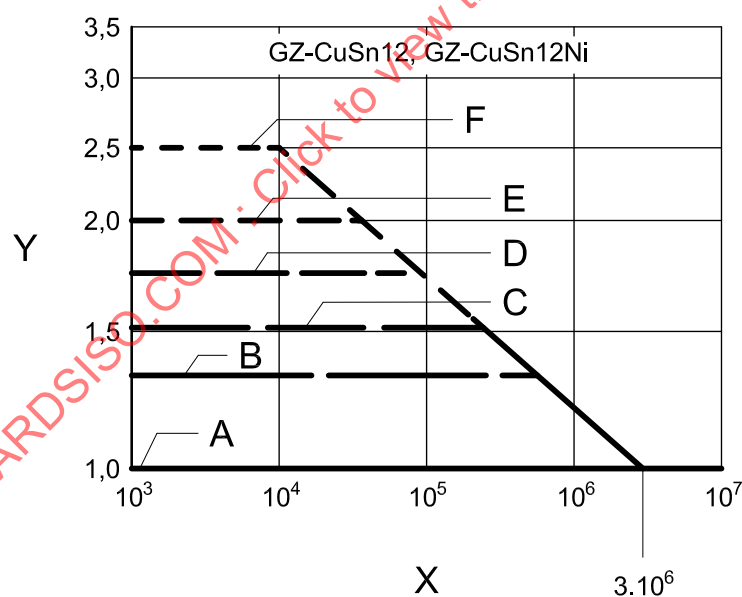
The life factor,  $Y_{NL}$ , is given numerically in Table 11.



**Key**

- X life factor  $Y_{NL}$   
Y number of stress cycles at the worm wheel  $N_L$

**Figure 13a — Life factor,  $Y_{NL}$ , in accordance with experiments: different materials,**



**Key**

- X life factor  $Y_{NL}$   
Y number of stress cycles at the worm wheel  $N_L$   
A deterioration to initial accuracy grade up to 7  
B deterioration to accuracy grade 8  
C deterioration to accuracy grade 9  
D deterioration to accuracy grade 10  
E deterioration to accuracy grade 11  
F deterioration to accuracy grade 12

**Figure 13b — Life factor,  $Y_{NL}$ , in accordance with experiments: copper-tin-bronze, with deterioration according to accuracy grade 7 to 12 (by analogy with DIN 3974) on pitch deviation.**



**Table 11 — Life factor as a function of the number of stress cycles,  $N_L$ , the material and the permissible accuracy grade**

Life Factor $Y_{NL}$	No. of stress cycles $N_L^{1)}$	Material / Accuracy grade
1,25	$< 8,3 \cdot 10^5$	GZ-CuSn12 and
$(3 \cdot 10^6 / N_L)^{0,16}$	$8,3 \cdot 10^5 \leq N_L \leq 3 \cdot 10^6$	GZ-CuSn12Ni2 with deterioration
1,0	$> 3,0 \cdot 10^6$	according accuracy grade DIN 8
1,5	$< 2,3 \cdot 10^5$	GZ-CuSn12 and
$(3 \cdot 10^6 / N_L)^{0,16}$	$2,3 \cdot 10^5 \leq N_L \leq 3 \cdot 10^6$	GZ-CuSn12Ni2 with deterioration
1,0	$> 3,0 \cdot 10^6$	according accuracy grade DIN 9
1,75	$< 9,5 \cdot 10^4$	GZ-CuSn12 and
$(3 \cdot 10^6 / N_L)^{0,16}$	$9,5 \cdot 10^4 \leq N_L \leq 3 \cdot 10^6$	GZ-CuSn12Ni2 with deterioration
1,0	$> 3,0 \cdot 10^6$	according accuracy grade DIN 10
2	$< 4 \cdot 10^4$	GZ-CuSn12 and
$(3 \cdot 10^6 / N_L)^{0,16}$	$4 \cdot 10^4 \leq N_L \leq 3 \cdot 10^6$	GZ-CuSn12Ni2 with deterioration
1,0	$> 3,0 \cdot 10^6$	according accuracy grade DIN 11,
2,5	$< 1 \cdot 10^4$	GZ-CuSn12 and
$(3 \cdot 10^6 / N_L)^{0,16}$	$1 \cdot 10^4 \leq N_L \leq 3 \cdot 10^6$	GZ-CuSn12Ni2 with deterioration
1,0	$> 3,0 \cdot 10^6$	according accuracy grade DIN 12,
2,0	$< 4,0 \cdot 10^4$	GZ-CuAl10 Ni
$(3 \cdot 10^6 / N_L)^{0,09}$	$4,0 \cdot 10^4 \leq N_L \leq 3 \cdot 10^6$	
1,0	$> 3,0 \cdot 10^6$	
2,5	$< 1,0 \cdot 10^4$	GGG-40
$(3 \cdot 10^6 / N_L)^{0,09}$	$1,0 \cdot 10^4 \leq N_L \leq 3 \cdot 10^6$	
1,0	$> 3,0 \cdot 10^6$	
2,0	$< 1,0 \cdot 10^3$	GG-25
$(3 \cdot 10^6 / N_L)^{0,16}$	$1,0 \cdot 10^3 \leq N_L \leq 3 \cdot 10^6$	
1,0	$> 3,0 \cdot 10^6$	
<sup>1)</sup> Number of stress cycles of worm wheel $N_L$ , see Equation (71)		

## 12.4 Adaptation of the calculation procedure to a specific test

If certain investigations have been carried out the values given in Table 10 can be replaced by the specific investigation values. The test results give the transferable torque as the damage limit. From this limiting values for the nominal shear stress  $\tau_{FG}$ , are derived according to Equation (150).

## 13 Temperature safety factor

### 13.1 Temperature safety factor for splash lubrication

With increasing temperatures, the life expectancy of the lubricant decreases rapidly. The additive decomposition is accelerated and the sealing rings could be damaged.

The operating temperature of a gear unit is dependent on the losses and design of case as such these calculations are intended as a guide when better data is not available.

The temperature safety factor is defined as follows:

$$S_T = \theta_{\text{Slim}} / \theta_S \geq S_{T\text{min}} \quad (157)$$

The oil sump temperature,  $\theta_S$ , is defined as is stipulated in 13.1.1 and the limiting oil sump temperature,  $\theta_{\text{Slim}}$ , is defined as in 13.1.2.

Minimum safety factor:

$$S_{T\text{min}} = 1,1 \quad (158)$$

### 13.1.1 Determination of oil sump temperature

#### a) Method A

Measurement of the oil sump temperature,  $\theta_S$ , at operating conditions (see Bibliography [22]).

#### b) Method B

Accurate thermodynamic analysis of the temperature during operation (see Bibliography [22]).

#### c) Method C

Usage limitations:

- centre distance from  $a = 63$  mm to  $a = 400$  mm
- rotational speeds from  $n_1 = 60$  mm<sup>-1</sup> to  $n_1 = 3000$  min<sup>-1</sup>
- gear ratio  $u = 10$  to  $u = 40$
- well ribbed housing made out of cast iron.

The oil sump temperature can be estimated as follows:

The use of these approximate equations for determining sump oil temperature may result in a calculated temperature variation of  $\pm 10$  K or even greater.

$$\theta_S = \theta_0 + \left( a_1 \cdot \frac{T_2}{\left( \frac{a}{63} \right)^3} + a_0 \right) \cdot a_2 \quad (159)$$

Oil sump temperature coefficients,  $a_1$   $a_0$  for housings with fan:

$$a_1 = \frac{3,9}{100} \cdot \left( \frac{n_1}{60} + 2 \right)^{0,34} \cdot \left( \frac{v_{40}}{100} \right)^{-0,17} \cdot u^{-0,22} \cdot (a - 48)^{0,34} \quad (160)$$

$$a_0 = \frac{8,1}{100} \cdot \left( \frac{n_1}{60} - 0,23 \right)^{0,7} \cdot \left( \frac{v_{40}}{100} \right)^{0,41} \cdot (a + 32)^{0,63} \quad (161)$$

**Oil sump temperature coefficients,  $a_1$   $a_0$  for housings without fan:**

$$a_1 = \frac{3,4}{100} \cdot \left( \frac{n_1}{60} + 0,22 \right)^{0,43} \cdot \left( 10,8 - \frac{v_{40}}{100} \right)^{-0,0636} \cdot u^{-0,18} \cdot (a - 20,4)^{0,26} \quad (162)$$

$$a_0 = \frac{5,23}{100} \cdot \left( \frac{n_1}{60} + 0,28 \right)^{0,68} \cdot \left( \left| \frac{v_{40}}{100} - 2,203 \right| \right)^{0,0237} \cdot (a + 22,36)^{0,915} \quad (163)$$

Factor  $a_2$  for mineral oils:

$$a_2 = 1 + \frac{9}{(0,012 \cdot u + 0,092) \cdot n_1^{0,5} - 0,745 \cdot u + 82,877} \quad (164)$$

Factor  $a_2$  for polyalphaolefines:

$$a_2 = 1 + \frac{5}{(0,012 \cdot u + 0,092) \cdot n_1^{0,5} - 0,745 \cdot u + 82,877} \quad (165)$$

Factor  $a_2$  for polyglycols:

$$a_2 = 1 \quad (166)$$

### 13.1.2 Limiting values

The limiting values of the oil manufacturer must be considered for the oil sump temperature.

Usually valid however is:

- for mineral oil  $\theta_{\text{Slim}} \cong 90 \text{ }^\circ\text{C}$ ,
- for polyalphaolefines  $\theta_{\text{Slim}} \cong 100 \text{ }^\circ\text{C}$
- for polyglycols  $\theta_{\text{Slim}} \cong 100 \text{ }^\circ\text{C}$  to  $120 \text{ }^\circ\text{C}$ . ( $100^\circ\text{C}$  is preferred)

### 13.2 Temperature safety factor for oil spray lubrication

The temperature safety factor for spray lubrication is calculated as follows:

$$S_T = P_K / P_V \geq S_{\text{Tmin}} \quad (167)$$

The total power loss,  $P_V$ , is defined as stipulated in 8.2 and the oil cooling capacity,  $P_K$ , with oil quantity,  $Q_{\text{oil}}$ , is defined as in 13.2.1.

Minimum safety factor:

$$S_{\text{Tmin}} = 1,1 \quad (168)$$

#### 13.2.1 Cooling capacity $P_K$

##### a) Method A

Measurement of the cooling capacity  $P_K$ , at operating conditions (see Bibliography [22]).

**b) Method B**

Accurate thermodynamic analysis of the cooling capacity, from entrance and exit temperature, during operation (see Bibliography [22]).

**c) Method C**

Valid for cooling capacity:

$$P_K = c_{oil} \cdot \rho_{oil} \cdot Q_{oil} \cdot \Delta\theta_{oil} \quad (169)$$

where,  $\rho_{oil}$ , is provided by manufacturer of the oil.

The usual specific heat capacity,  $c_{oil}$ , for all type of oils is:

$$c_{oil} = 1,9 \cdot 10^3 \text{ in Ws / (kg} \cdot \text{K)} \quad (170)$$

The temperature difference,  $\Delta\theta_{oil}$ , of the difference between exit and entrance temperature of the oil.

See Figure 14.

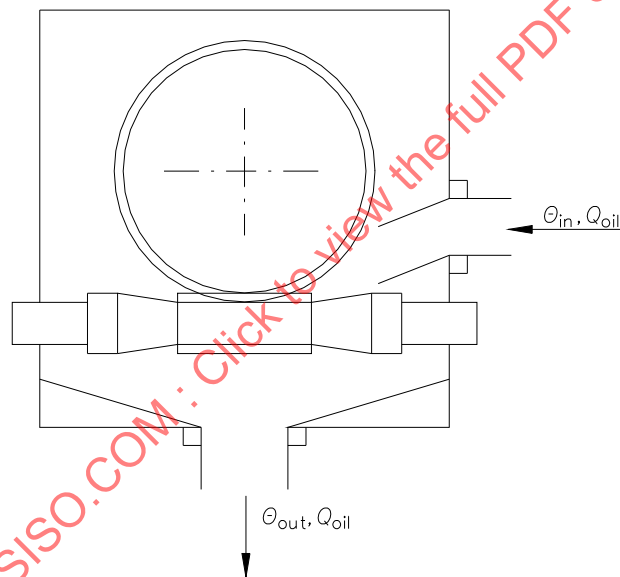


**Figure 14 — Definition for cooling capacity**

$$\Delta\theta_{oil} = \theta_{out} - \theta_{in} \quad (171)$$

$Q_{oil}$  and  $\Delta\theta_{oil}$  must be agreed upon in co-operation with the manufacturer of the lubricating system.

( $\Delta\theta_{oil}$  without cooler amount to 3 ... 5 K, with cooler 10 ... 20 K).

## 14 Determination of the wheel bulk temperature

The wheel bulk temperature is required for determination of the wear intensity (see Clause 5).

### 14.1 Wheel bulk temperature with splash lubrication

#### a) Method A

Measurement of the wheel bulk temperature at operating conditions.

#### b) Method B

Accurate thermodynamic analysis of the wheel bulk temperature at operating conditions.

#### c) Method C

Calculation of the wheel bulk temperature, see Bibliography [24]:

$$\theta_M = \theta_S + \Delta\theta \quad (172)$$

The oil sump temperature,  $\theta_S$ , is determined as is stipulated in 13.1.1.

Calculation of the wheel tooth temperature in excess of the oil sump temperature:

$$\Delta\theta = \frac{1}{\alpha_L \cdot A_R} \cdot P_{VZ} \quad (173)$$

The meshing power loss,  $P_{VZ}$ , is derived according to Equation (105) or Equation (106), the heat transition coefficient,  $\alpha_L$ , according to Equation (175) or Equation (176) and the dominant cooled surface of the gear set according to Equation (174).

Dominant cooled surface of the gear set,  $A_R$ :

$$A_R = b_{2R} \cdot d_{m2} \cdot 10^{-6} \quad (174)$$

Heat transition coefficient  $\alpha_L$ :

$$\begin{aligned} \alpha_L &= c_K \cdot (1940 + 15 \cdot n_1) \text{ for } n_1 \geq 150 \text{ min}^{-1} \\ \alpha_L &= c_K \cdot 4190 \text{ for } n_1 < 150 \text{ min}^{-1} \end{aligned} \quad (175)$$

where  $c_K = 1$  for immersed worm wheel

$c_K = 0,8$  for not immersed worm wheel.

### 14.2 Wheel bulk temperature with spray lubrication

#### a) Method A

Measurement of the wheel bulk temperature at operating conditions.

#### b) Method B

Accurate thermodynamic analysis of the wheel bulk temperature at operating conditions.

#### c) Method C

Calculation of the wheel bulk temperature, see Bibliography [24]:

$$\theta_M = \theta_{oil} + 16 \cdot K_n \cdot K_v \cdot K_S \cdot P_{VZ} / 1000 \quad (176)$$

Rotational speed factor  $K_n$ :

$$\begin{aligned} K_n &= (\mu \cdot 72,5 / n_1)^{0,35} & \text{for } n_1 \geq 150 \text{ min}^{-1} \\ K_n &= (\mu \cdot 72,5 / 150)^{0,35} & \text{for } n_1 < 150 \text{ min}^{-1} \end{aligned} \quad (177)$$

Viscosity factor  $K_v$ :

$$K_v = (\nu_E / 55)^{0,35} \quad (178)$$

The kinematic viscosity  $\nu_E$  must be determined by Equation (74) or from the viscosity-temperature characteristic line of the lubricant at the spray temperature  $\theta_{oil}$ .

Size factor  $K_S$ :

$$K_S = (160/a)^{0,6} \quad (179)$$

Meshing power loss  $P_{Vz}$ , as stipulated in 8.4.

STANDARDSISO.COM : Click to view the full PDF of ISO/TR 14521:2010

## **Annex A**

(informative)

### **Notes on physical parameters**

The research into the physical causes for worm wheel damages have not yet been sufficiently developed in order to be able to include all the determinant factors in a calculation for the load capacity. This applies especially to the wear load capacity and the surface durability (pitting). Parameters are used for the assessment of the load capacity (e.g. mean contact stress for surface durability). According to present day knowledge, other influential factors such as coefficient of friction, velocity and size of slip etc. cannot yet be directly included in the calculation of load capacity.

Despite these deficiencies the parameters are useful when describing the worm drive behaviour, as the limiting values are determined on the basis of running tests with worm gear sets.

With present day computers it is possible to calculate a maximum value for hertzian stress in place of the mean value. This maximum value is then, only acting at one contact point. Finite element methods of today allow calculations such as those required to solve contact problems. These programs are also applicable to considerations such as the shear stresses and the stresses induced by increased flank temperature.

This clearly shows that gear optimisation by calculating the load capacity based on these parameters can only be used in a limited manner and that caution is advised.

## Annex B (informative)

### Methods for the determination of the parameters

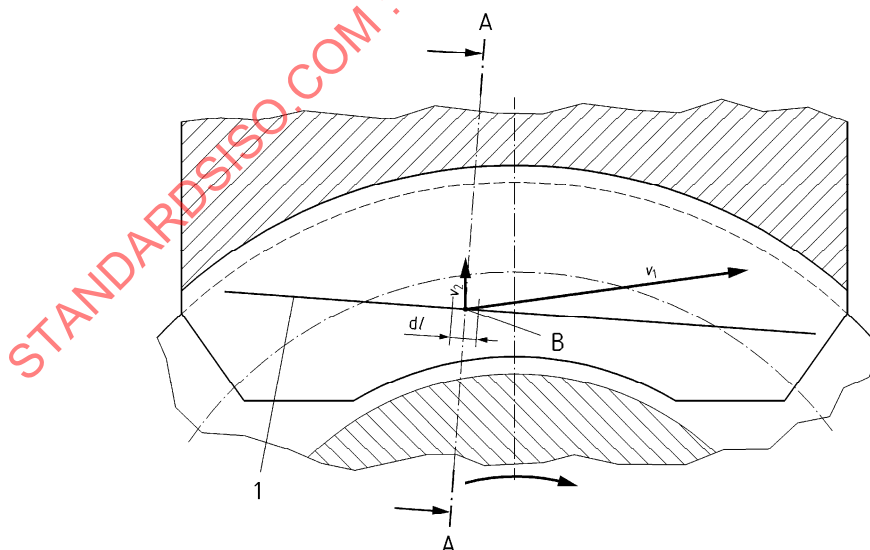
Due to the complex geometrical conditions it is not possible to give a complete general solution, e.g. for the hertzian stress of a worm drive. The parameters for the calculation of contact lines can be determined by means of EDV - programming. Approximate solutions can also be used for these parameters. Briefly outlined next is the procedure for the calculation of the parameters with the aid of computer program according to Bibliography [32] and [36].

With the equations for the generatrix of the worm flanks, i.e. for flank form I the transverse involute, the contact lines of the worm and worm wheel are initially calculated. For this purpose, the initial position of a worm tooth is sought. Subsequently the worm is rotated by a defined angle, until no contact between the worm tooth and wheel exists. In general about twenty four worm positions are sufficient. Thus the total range of contact is accounted for and Figure D.2 shows the development of the contact lines as an example.

For each contact point (in general about 2000 to 3000) the following parameters must be calculated:

- the velocities ( sum of two surface velocities, sliding velocity etc.);
- hertzian stress and reduced radius of curvature in compliance with Bibliography [32] and [36] for example;
- lubricant film thickness in compliance with EHL (Elasto Hydrodynamic Lubrication) – theory;
- local sliding path. As a rule, it is sufficient to determine a mean parameter for the total meshing zone.

This contact line belongs to a certain position of the worm and to a certain position of the worm wheel. While turning worm and worm wheel, this contact line moves on the worm wheel. For analysing the behaviour of the contact between worm wheel and worm along the contact line, it is useful, to divide the contact line into infinitesimal pieces, as indicated in Figure B.1.

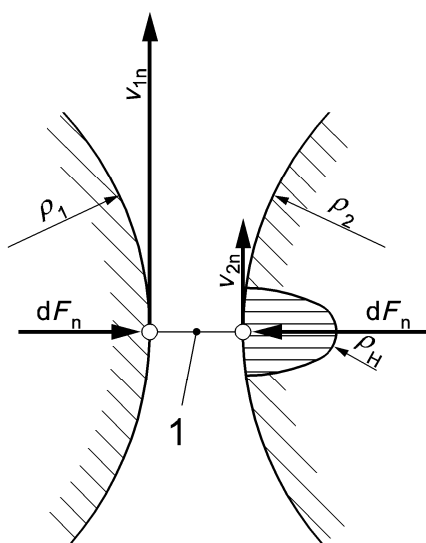


#### Key

- 1 contact line

**Figure B.1 — Contact line on a worm wheel**



**Key**

1 contact line

**Figure B.2 — Section normal to contact line (section A-A)**

Taking one of these pieces of the contact line and looking at a plane normal to this contact line, it is possible to see the flanks of worm and worm wheel as shown in Figure B.2. In the contact point B, the main radii of curvature  $\rho_1$  and  $\rho_2$  of worm and worm wheel can be determined. As a first approximation the actual profile lines of worm and worm wheel can be built by equivalent cylinders with the radii of curvature  $\rho_1$  and  $\rho_2$ . These radii of curvature are important for the calculation of the hertzian stress along the concerning piece of the contact line. It is also possible to calculate the speeds of the flanks  $v_1$  and  $v_2$  of the worm and the worm wheel in the contact point B. The knowledge of these speeds is important in order to calculate the lubricant film thickness along the concerning piece of the contact line. The calculation of the speeds takes place in a tangential plane, that touches the flank of the worm as well as the flank of the worm wheel. The formula for the hertzian stress of a piece of the contact line is:

$$p_H = \sqrt{\frac{dF \cdot E_{red}}{2 \cdot \pi \cdot dl \cdot \rho_{red}}} \quad (B.1)$$

$$\rho_{red} = \frac{\rho_1 \cdot \rho_2}{\rho_1 + \rho_2} \quad (B.2)$$

$dF$  is the force transmitted by the piece of the contact line

$E_{red}$  is the equivalent E-module

$dl$  is the length of the piece of the contact line

$\rho_{red}$  is the equivalent radius of curvature

It is assumed that the hertzian stress is constant along the contact line. Otherwise, strong wear would appear at pieces of the contact line with higher stress and lead to a relief. With this assumption, of a constant hertzian stress along the contact line, it is possible to resolve the relationship stated above with respect to the force vector  $d\vec{F}$ . The force vector  $d\vec{F}$  can be calculated according Equation (B.3)

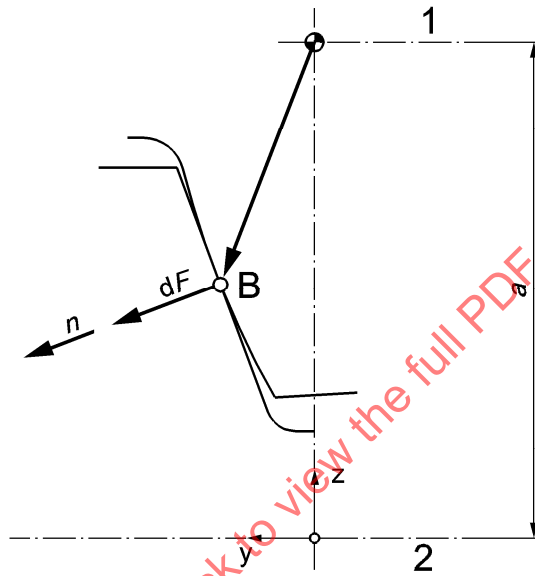
$$d\vec{F} = p_H^2 \cdot \frac{2\pi}{E_{red}} \cdot \rho_{red} \cdot dl \cdot \vec{n} \quad (B.3)$$

$d\vec{F}$  is the force vector normal to the flanks of the worm wheel and the worm, or expressed in other words normal to the tangential plane mentioned earlier.  $\vec{n}$  is the normal vector, that is normal to the two tooth flanks as well as to the tangential plane. Viewing a parallel section (offset plane see ISO 1122-2) leading through the contact point B as shown in Figure B.3 it is possible to represent the apparent torque at the worm wheel  $T_2$  like:

$$T_2 = 10^{-3} \cdot \int_l (d\vec{F} \times \vec{r}) \cdot \vec{e}_x \cdot dl \quad (\text{B.4})$$

$\vec{e}_x$  is an unit vector pointing in direction of the x-axis.

In this case  $\vec{r}$  is the radius from the axis of the worm wheel to the contact point B.



**Key**

- 1 axis of worm wheel
- 2 axis of worm

**Figure B.3 — Parallel section through the worm gear set**

NOTE Only projection of  $\vec{n}$  and  $d\vec{F}$  are represented in Figure B.3.

Substituting the force vector along to the infinitesimal piece of the contact line with the length of  $dl$  calculated in Equation (B.5) following results:

$$T_2 = p_H^2 \cdot \frac{2 \cdot 10^{-3} \cdot \pi}{E_{\text{red}}} \int_l (\rho_{\text{red}} \cdot \vec{n} \times \vec{r}) \cdot \vec{e}_x \cdot dl \quad (\text{B.5})$$

In this case the integration takes place over the length of all contact lines that are in mesh at the same time. Often there are three teeth in engagement and so the integration has to take place to account for all three contact lines. With the equation of the torque  $T_2$  it is possible to determine the hertzian stress. For the hertzian stress  $p_H$  following is valid:

$$p_H = \frac{4}{\pi} \cdot \sqrt{\frac{T_2 \cdot E_{\text{red}} \cdot 10^3}{a^3} \cdot \left[ \frac{\pi}{32} \cdot a^3 \cdot \frac{1}{\int_l (\rho_{\text{red}} \cdot \vec{n} \times \vec{r}) \cdot \vec{e}_x \cdot dl} \right]} \quad (\text{B.6})$$

The expression of Equation (B.7) put in square brackets consists only of geometrical values. The integral can only be solved by computer programs. This calculation sums up the values to be integrated in dependence of each piece of the contact lines. The value put in square brackets is named  $p^*$ . When  $p^*$  is known, it is now possible to calculate the hertzian stress  $p_H$  from the torque, the equivalent Modulus of elasticity and the centre distance. This hertzian stress is now decisive for a certain position between worm and worm wheel and the contact lines that are in engagement at the same time. When turning worm and worm wheel a little bit further, the contact lines are moving, and those new contact lines lead to a new hertzian stress  $p_H$ . For further calculations it should be suitable to use mean value of the hertzian stress of all investigated positions of the worm. This mean hertzian stress  $p_{Hm}$  must be calculated by:

$$p_{Hm} = \frac{4}{\pi} \cdot \sqrt{\frac{T_2 \cdot E_{red} \cdot 10^3}{a^3}} \cdot p_m^* \quad (B.7)$$

with:

$$p_m^* = \frac{\pi}{32} \cdot \frac{a^3}{\int_l (\rho_{red} \cdot \vec{n} \times \vec{r}) \cdot \vec{e}_x \cdot dl} \quad (B.8)$$

$p_m^*$  mean value of the geometrical value  $p^*$  explained before

Experimental investigations concerning wear and pittings have shown that this mean hertzian stress  $p_{Hm}$  has a strong influence. For the calculation of the hertzian stresses at the worm wheel, the acting torque  $T_2$ , the equivalent modulus of elasticity  $E_{red}$  and the centre distance  $a$  are known. The value of  $p_m^*$  can be calculated by using the formula stated in this standard.

As well as shown here for the hertzian stress, the mean lubricant film thickness  $h_{min m}$  and the mean sliding path  $s_{gm}$  can be calculated.

The usual parameters gained in this manner for the hertzian stress, minimum lubricant film thickness and sliding path are non-dimensional, they have the advantage that they are only dependant on the gearing geometry. Therefore if these parameters are known for a certain gearing, the hertzian contact stress, the lubricant film thickness and the sliding path, can be easily determined for every possible loading, rotational speed, and lubricant, corresponding to that gearing.

## Annex C (informative)

### Lubricant film thickness according to EHL - theory

#### C.1 Principe of calculation

In accordance with Dowson and Higginson [19], the minimum lubricant film thickness,  $h_{\min}$ , between the flanks (localised value for one contact point) can be calculated as follows:

$$h_{\min} = 1,6 \cdot \alpha^{0,6} \cdot \eta_{0M}^{0,7} \cdot E_{\text{red}}^{0,03} \cdot \rho_{\text{red}}^{0,43} \cdot (v_{\Sigma n}/2)^{0,7} / (dF/dl)^{0,13} \quad (\text{C.1})$$

where:

$h_{\min}$  is in  $\mu\text{m}$

$E_{\text{red}}$  is in  $\text{N/m}^2$

$\rho_{\text{red}}$  is in  $\text{m}$

$dF/dl$  is in  $\text{N/m}$

A determinant influence factor is the dynamic viscosity,  $\eta_{0M}$ , of the lubricant at ambient pressure and bulk temperature of the worm wheel. Due to temperatures of the worm wheel in large excess of the oil, the oil viscosity has to be considered at the wheel bulk temperature.

The value,  $h_{\min m}$ , is calculated on the basis of local values for  $h_{\min}$ .  $h_{\min m}$  is the mean minimum lubricant film thickness over the entire meshing zone.

As to the significance of the mean value  $h_{\min m}$ , the following is stated: ( $\vec{v}_{\Sigma} = \vec{v}_1 + \vec{v}_2$ )

For A, I, N, K profiles a zone exists around the centre of the face width of the worm wheel where the sum of the two velocities  $v_{\Sigma}$ , becomes zero and the conditions of the EHL - theory [33], are no longer fulfilled. Eventually, it is dubious if the development of a mean value is at all permissible in order to really understand the physical happenings. The above mentioned criteria show that the calculation of a lubricant film thickness cannot be seen as a physical determinant.

According to the evaluation of test results, the integral usage of the mean value,  $h_{\min m}$ , is at least as a relevant parameter.

#### C.2 Guideline to calculate $h^*$

For  $h^*$  see 7.3.2.

In the following, units are according to Table 1.

$$h_{\min m} = \frac{1}{\sum_{St} \cdot \sum_{Bl} dl} \cdot \sum_{St} \cdot \sum_{Bl} (h_{\min} \cdot dl) \quad (\text{C.2})$$

From which we can determine:

$$h^* = \frac{(1000)^{-0,5}}{\sum_{St} \cdot \sum_{Bl} dl} \cdot \sum_{St} \cdot \sum_{Bl} (h_{\min} \cdot dl) \cdot \frac{T_2^{0,13}}{21 \cdot c_\alpha^{0,6} \cdot \eta_{OM}^{0,7} \cdot n_1^{0,7} \cdot a^{1,39} \cdot E_{\text{red}}^{0,03}} \quad (\text{C.3})$$

After simplification we get:

$$h^* = \frac{(1000)^{-0,5}}{\sum_{St} \cdot \sum_{Bl} dl} \cdot \sum_{St} \cdot \sum_{Bl} \left( 1,6 \cdot \rho_{\text{red}}^{0,43} \cdot \left( \frac{v_{\Sigma h}/2}{dF/dl} \right)^{0,7} \cdot dl \right) \cdot \frac{T_2^{0,13}}{21 \cdot n_1^{0,7} \cdot a^{1,39}} \quad (\text{C.4})$$

but from C.3 we can obtain:

$$\frac{dF}{dl} = \frac{2 \cdot \pi}{E_{\text{red}}} \cdot p_H^2 \cdot \rho_{\text{red}} \quad (\text{C.5})$$

but:

$$p_H = \sqrt{T_2 \cdot \frac{E_{\text{red}}}{2 \cdot 10^{-3} \cdot \pi} \cdot \frac{1}{\int_l (\rho_{\text{red}} \cdot \vec{n} \times \vec{r}) \cdot \vec{e}_x \cdot dl}} \quad (\text{C.6})$$

$$\text{so: (1000 appears)} \quad \frac{dF}{dl} = T_2 \cdot \frac{1000}{\int_l (\rho_{\text{red}} \cdot \vec{n} \times \vec{r}) \cdot \vec{e}_x \cdot dl} \cdot \rho_{\text{red}} \quad (\text{C.7})$$

$$h^* = \frac{(1000)^{-0,63}}{\sum_{St} \cdot \sum_{Bl} dl} \cdot \sum_{St} \cdot \sum_{Bl} \left( 1,6 \cdot \rho_{\text{red}}^{0,3} \cdot \left( \frac{v_{\Sigma h}}{2 \cdot n_1} \right)^{0,7} \cdot \left( \int_l (\rho_{\text{red}} \cdot \vec{n} \times \vec{r}) \cdot \vec{e}_x \cdot dl \right)^{0,13} \cdot dl \right) \cdot \frac{1}{21 \cdot a^{1,39}} \quad (\text{C.8})$$

## Annex D (informative)

### Wear path definitions

The wear path,  $s_W$ , covered during life is calculated from the number of stress cycles of the wheel  $N_L$ , and the sliding path of the worm flank within the hertzian contact on the wheel flank.

$$s_{Wm} = s_{gm} \cdot N_L \quad (D.1)$$

Figure B.2 shows the contact line that is normal to the flanks of the worm and the worm wheel.

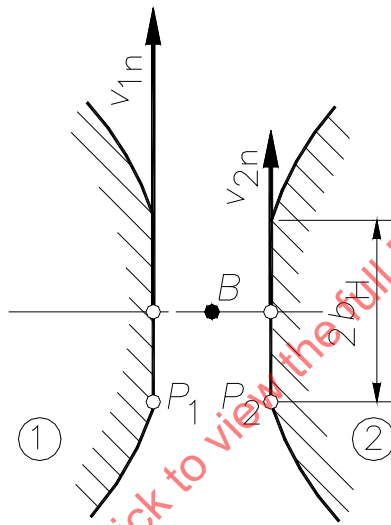


**Figure D.1 — Contact point B of the flanks of the worm and the worm wheel**

In opposite to Figure B.2, the flanks are shown flattened because of the hertzian stress in Figure D.1. The width of the flattening amounts to  $2 \cdot b_H$ . Further the actual speeds of the two flanks  $\vec{v}_{1n}$  and  $\vec{v}_{2n}$  can be seen. First it should be determined, on which local sliding path  $s_{gB}$  a point  $P_2$ , that belongs to the flank of the worm wheel in the plane of the flattening moves relatively to the flank of the worm. A stationary movement of the two equivalent flanks relatively to the contact lines is required. In reality, of course, the movements are absolutely non-stationary because the position of the contact lines and the position of the curvatures of the both equivalent cylinders change continuously. With this implied stationary condition the flattening at the worm and the worm wheel is timewise constant. A point of the worm wheel  $P_2$  has the speed  $\vec{v}_{2n}$  while moving in the flattening plane. The time of contact results from the following equation:

$$t_{\text{contact}} = 2 \cdot \frac{b_H}{\vec{v}_{2n}} \quad (D.2)$$

Normally only the worm wheel of a worm gear set shows wear, as the worm consists of hardened steel and the worm wheel of bronze. Therefore most important for the wear of the worm wheel is the sliding path of the point  $P_2$  of the worm wheel in relation to a point  $P_1$  of the flank of the worm. The affiliated local sliding path  $s_{gB}$  results from the sliding speed  $\vec{v}_{gB}$  between the two points  $P_1$  and  $P_2$  and the time of contact  $t_{\text{contact}}$ . Then for the local sliding path following results:

$$s_{gB} = |\vec{v}_{gB}| \cdot t_{\text{contact}} \quad (D.3)$$

The sliding speed  $\vec{v}_{gB}$  is the difference between the speeds  $\vec{v}_1$  and  $\vec{v}_2$  projected in the common tangent plane of contact. With this the local sliding path can be calculated with:

$$s_{gB} = |\vec{v}_1 - \vec{v}_2| \cdot t_{\text{contact}} \quad (\text{D.4})$$

Together with Equation (D.2) follows for the local sliding path:

$$s_{gB} = \frac{|\vec{v}_{gB}|}{\vec{v}_{2n}} \cdot 2 \cdot b_H \quad (\text{D.5})$$

For a worm gear set the sliding speed  $\vec{v}_{gB}$  has to be built by the following equation because the flanks of the worm and the worm wheel is not only moving normal to the contact line but also in opposite directions on the contact line:

$$\vec{v}_{gB} = \vec{v}_1 - \vec{v}_2 \quad (\text{D.6})$$

The vectors  $\vec{v}_1$  and  $\vec{v}_2$  are the speeds of the flanks of the worm and the worm wheel in the tangential plane between the two flanks for a certain contact point.

The local sliding paths are calculated for all infinitesimal neighbouring contact points. Then the mean value of all sliding paths can be calculated. This mean value is named mean sliding path  $s_{gm}$ .

$$s_{gm} = s^* \cdot \sigma_{Hm} \cdot \frac{a}{E_{red}} \quad (\text{D.7})$$

$\sigma_{Hm}$  is the mean hertzian stress

$a$  is the centre distance

$E_{red}$  is the equivalent modulus of elasticity

$s^*$  is the parameter for the mean sliding path

$s^*$  is as well as  $p_m^*$  a pure geometrical value that can be calculated in a similar way with computer programs. In general, it is sufficient to calculate  $s^*$  with approximation equations that can be found in this Technical Report.

The local sliding path appears each time when a tooth comes in contact again. The wear path is increased with the number of stress cycles as well as the number of the revolutions of the worm wheel.

Many experimental investigations have shown that the wear path  $s_W$  is an important value for the behaviour of the wear of a worm gear set.

As an example, the procedure for the calculation of the mean sliding path,  $s_{gm}$ , is shown here; it is the integral mean value of the total local sliding paths  $s_{gB}$  over the total meshing zone. See Figure D.2.

For the mean sliding path,  $s_{gm}$ , the following mean values are calculated:

- the mean local sliding path,  $s_{gB}$ , in each contact line section (dl) between two contact points;
- mean value over the contact lines (BL) which are simultaneously present at the worm position;
- mean value between the calculated position (St) of a load cycle.

Thus the mean value for the contact is:

$$s^* = \frac{1}{\sum_{St} \cdot \sum_{Bl} dl} \cdot \sum_{St} \cdot \sum_{Bl} (s_{gB} \cdot dl) \cdot \frac{E_{red}}{a} \cdot \frac{1}{\sigma_{Hm}} \quad (D.8)$$

$St$ : number of calculated position.

$BL$ : number of contact lines for one calculated position. Figure B.1 shows a contact line on the worm wheel.

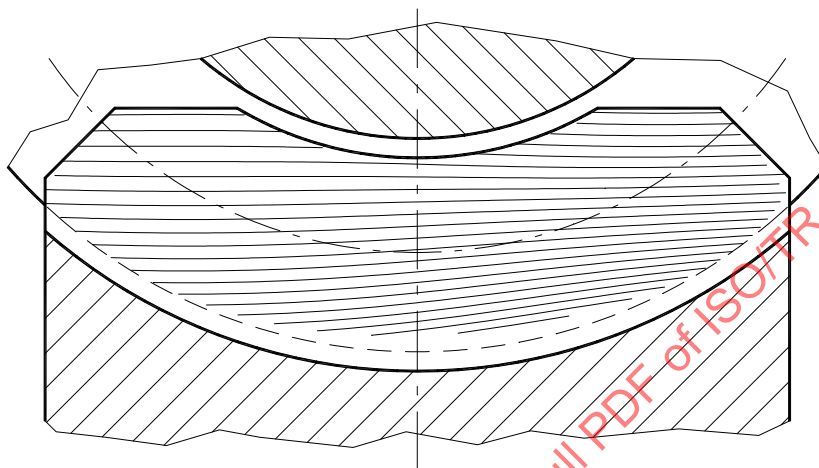


Figure D.2 — Example of contact line calculation (projection in wheel plane)



## Annex E (informative)

### Notes on calculation wear

The calculation procedure described here is based on tests run with bronze wheels and oil, both of which are from a single batch. Experience to date, shows that considerable influences can be associated with material and oil. Test and operational experience show that wear values undergo a very large scattering and classification of unknown lubricant, even with known base oils, is only possible within limits. With the wear relationship investigation stated here, only the investigated pairings are, in principle, calculable.

Furthermore the following restrictions can be observed:

- The calculation is only valid for constant power and gears that have been run-in. Wear peaks due to overloading or impermissible oil temperatures are **not** considered.
- The calculation is only valid for case hardened and ground worms and  $Ra_1 \leq 0,5 \mu\text{m}$ ; larger roughness' can cause considerable increases in the wear, especially during the run-in.

## **Annex F** (informative)

### **Notes on tooth root strength**

The calculations only apply to the root strength of the wheel teeth when coupled with worms made of 16MnCr5 steel case hardened. During experiments concerning endurance limit and the region of time strength, the wheel teeth tend to break in the case of gear pairs with bronze wheel; in the case of wheels made of grey cast and nodular cast materials, the worm threads break.

The endurance strengths for the plastifying materials (CuSn - bronzes) are already partially in the plastic range. If small plastic deformations are permissible, these values can be calculated. Otherwise reduced strength values should be used. Average values for perfect structures have been taken as the basis for the yield point. The time strength of these wheels can be understood as a sort of damage line which runs in the plastic range and is limited by the definition of a permissible accuracy grade deterioration (plastic deformation) of the worm wheel.

For the more brittle and harder aluminium bronze alloy, the difference between the plasticity and elasticity is smaller.

For grey cast iron and nodular iron the endurance and time strength values lie in the elastic region.

When determining the shear stress the reduction of the tooth root chord due to abrasive wear can be taken into account, since this weakens the wheel tooth. The wheel tooth can also be weakened by a high pitting incurrence. This however can not be taken into account due to inconclusive calculations.

## Annex G (informative)

### The utilisation of existing tooling for machining of worm wheel teeth

It is usual for the designer, knowing the ratio required in terms of the number of threads in the worm  $z_1$  and the number of teeth in the worm wheel  $z_2$  and the centre distance  $a$ , to establish the diameter factor  $q_1$  prior to the module  $m_{x1}$ . This is due to the influence of  $q_1$  on the reference diameter of the worm and its proportions relative to the required stiffness and diameters to each side of the threads.

When a satisfactory  $q_1$  value is established the module can be determined from:

$$m_{x1} \approx \frac{2 \cdot a}{z_2 + q_1} \quad (\text{G.1})$$

This would complete the proposed designation:  $z_1/z_2/q_1/m_{x1}$

There are occasions where the gear manufacturer can have a stock of hobs or cutters which are available for utilisation in the machining of worm wheels for which they were not originally produced and yet may be suitable for use in other centre distances and ratios.

This is sometimes possible where the diameter factor and module of a hob approximate to those of the worm, the number of threads, hand and pressure angle, and with a modification to the reference diameter of the worm wheel the number of teeth required can be accommodated within the new centre distance.

In BS 721-2 there is guidance in checking the  $z_1$ ,  $q_1$ ,  $m_{x1}$ , values of the hob against the limits of the resulting modification. This is contained in 6.1 and 6.7 which provide methods of obtaining the allowable  $a_{\max 0} - a_{\min 0}$  and  $m_{\max 0} - m_{\min 0}$  values respectively.

Using the new  $z_2$  value with the hob  $z_1$ ,  $q_0$ , and  $m_{x0}$  values enables a check to be made that, the new centre distance falls within the established tolerance, or the limiting values of axial module encompass the existing  $m_{x0}$  of the hob.

The method proposed is as follows:

— Limiting values of centre distance for given values of  $a$ ,  $z_1$ ,  $z_2$ , and  $q_0$  are as follows:

$$a_{\max 0} = 0,5 \cdot m_{x0} \cdot (z_2 + q_0 + 2 \cdot x_{2\max}) \quad (\text{G.2})$$

where  $x_{2\max}$  is as given in Figure G.1.

$$a_{\min 0} = 0,5 \cdot m_{x0} \cdot (z_2 + q_0 - 2 \cdot x_{2\min}) \quad (\text{G.3})$$

where  $x_{2\min}$  is as given in Figure G.2.

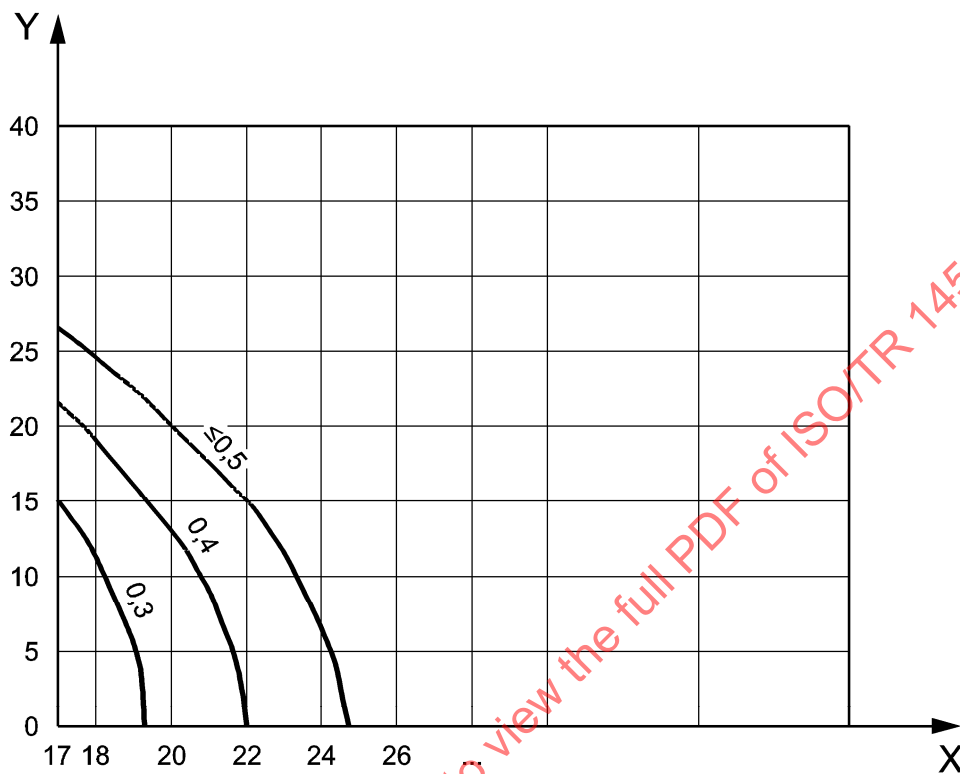
— Limiting values of axial module for given values of  $a$ ,  $z_1$ ,  $z_2$ , and  $q_0$  are as follows:

$$m_{\max 0} = \frac{2 \cdot a}{z_2 + q_0 - 2 \cdot x_{2\min}} \quad (\text{G.4})$$

$$m_{\min 0} = \frac{2 \cdot a}{z_2 + q_0 + 2 \cdot x_{2\max}} \quad (\text{G.5})$$

In order to use Figures G.1 and G.2 it is necessary to obtain the lead angle of the hob which can be found from:

$$\tan \gamma_1 = \frac{z_1}{q_0} \quad (G.6)$$



**Key**

X number of teeth  $z_2$   
Y lead angle  $\gamma_1$  in degrees

**Figure G.1 — Maximum value of addendum modification coefficient ( $x_{2max}$ )**